On Quantum Thermodynamics of Coupled Light-Matter Systems

Diplomarbeit von
Gerald Waldherr

06.10.2009

Hauptberichter: Günter Mahler
Mitberichter: Hans-Rainer Trebin

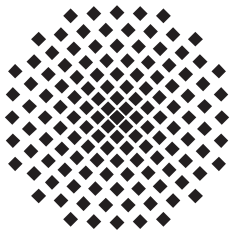

1. Institut für Theoretische Physik
Universität Stuttgart
Pfaffenwaldring 57, 70550 Stuttgart

Ehrenwörtliche Erklärung

Ich erkläre, dass ich diese Arbeit selbständig verfaßt und keine anderen als die angegebenen Quellen und Hilfsmittel benutzt habe.

Stuttgart, 06.10.2009 *Gerald Waldherr*

Contents

1 Introduction

Phenomenological thermodynamics was mainly developed in the 17-19th century. Based on very few, intuitively observed state variables, many characteristics of large systems can be described, independently of the details of the system. One main finding was that after a long enough time, every system reaches an equilibrium state, where the state variables do not alter any more. A fundamental problem is explaining how thermodynamical behavior results from the underlying dynamics, which can only be achieved by introducing further assumptions (e.g. quasi-ergodicity and coarse graining in classical mechanics).

In [16, 33, 19], considerable success has been made in explaining how thermodynamical behavior emerges from quantum mechanics. The reason for this emergence is mainly associated with embedding of an observed system in some kind of environment, and to the thereby occurring entanglement. For entangled systems, a mixed state of one subsystem naturally results from quantum mechanics without further assumptions. For a system which is small compared to its environment, the reduced state of the system is approximately the same for almost all states of the combined system (system + environment). This feature is called typicality, and applies even to systems as small as one spin. Under certain conditions, the reduced state is in accord with classical thermostatistics.

Recently, there has been growing interest in thermodynamics of coupled light-matter systems [40, 5, 47], where the energy stored in a harmonic oscillator (representing one mode of the radiation field) is used to operate a heat pump. In this thesis, I investigate the behavior of a closed "laser"-model consisting of one oscillator coupled to a finite spin network. The main questions address the exact state of the oscillator during the evolution for different initial states, the separation of the energy flows into heat and work, and optical coherences.

There are different approaches on how to separate energy flows into heat and work in quantum mechanics [1, 4, 46]. The problem in [1, 4] is that it is unclear how to apply the definitions for heat and work to internal energy flows within closed systems. In this thesis, I use the definitions given by the so called LEMBAS-scheme described in [46].

In quantum optics, the state of the radiation field generated by a laser is assumed to be a coherent state [18]. This belief was questioned by K. Mølmer in [30], where he claims that optical coherences should not exist in common laser sources, meaning that the expectation values of the field amplitude operators vanish.

Another point I investigate is irreversibility and the arrow of time in quantum systems subject to unitary dynamics. This phenomenological observed behavior has been questioned by the Loschmidt paradox [25], namely that the underlying dynamics are invariant under time reversal: By reversing the dynamics, the system should evolve back into the initial state. This paradox can be solved by assuming that the control over

the system needed for the reversal is limited. A further important aspect leading to the arrow of time is "coarse-grained" observation of the system. There is an ongoing debate on such time reversal operations and the arrow of time [14, 11, 10, 26].

In chapter 2, I will give an overview over the theoretical basics, which are necessary for my diploma thesis. They cover the fields of quantum mechanics [7, 8], quantum optics [41, 17, 12] and thermostatistics [39, 16]. In chapter 3, a laser model subject to pure Schrödinger-dynamics and its temporal evolution for different initial states is presented. The following chapter 4 deals with the optical coherences and with the heat and work flows within the model. In chapter 5, the emergence of irreversibility in quantum system is discussed using recent results of quantum thermodynamics and numerical studies.

Part of this work will be published in [44, 43].

2 Theoretical Basics

2.1 Quantum Mechanics

Here, I will briefly introduce the quantum-mechanical concepts. For more detailed information see [7, 8].

2.1.1 Schrödinger Equation

In non-relativistic quantum mechanics, the Schrödinger equation describes the dynamics of a closed system:

$$\mathrm{i}\hbar\frac{\mathrm{d}}{\mathrm{d}t}|\psi(t)\rangle = \hat{H}|\psi(t)\rangle. \tag{2.1}$$

$|\psi(t)\rangle$ is a vector with norm one describing the state of the system. All state vectors belong to a vector space called Hilbert space $\mathcal{H}$. Measureable physical quantities are given by hermitian operators (called observables) acting in the Hilbert space. $\hat{H}$ is called the Hamiltonian and is associated with the total energy of the system. For a non-autonomous system $\hat{H}$ could be explicitly time-dependent. Any classical system can be described in quantum mechanics by suitable symmetrizing the classical Hamilton function and replacing the canonical variables q_i and p_i by the operators $\hat{q}_i$ and $\hat{p}_i$ with the canonical commutation relations

$$[\hat{q}_i, \hat{q}_j] = [\hat{p}_i, \hat{p}_j] = 0, \tag{2.2}$$
$$[\hat{q}_i, \hat{p}_j] = \mathrm{i}\hbar\delta_{ij}. \tag{2.3}$$

In this theoretical scheme observations are not yet included. As a remedy one needs additional postulates: A measurement of an observable $\hat{A}$ can only yield one of its eigenvalues a, according to

$$\hat{A}|a_i\rangle = a|a_i\rangle. \tag{2.4}$$

After the measurement of a, the state of the system is projected onto the subspace spanned by all eigenvectors $|a_i\rangle$ with eigenvalue a. An important quantity concerning observables is the expectation value

$$\langle\hat{A}\rangle_\psi = \langle\psi|\hat{A}|\psi\rangle, \tag{2.5}$$

which is the weighted mean value of all possible results of a measurement of $\hat{A}$.

2.1.2 Evolution Operator

Because the transformation between an initial state $|\psi(t_0)\rangle$ and the state $|\psi(t)\rangle$ (obtained by the Schrödinger equation for an arbitrary time t) is linear, there exists a linear operator $\hat{U}(t_0, t)$, which is called the evolution operator, such that

$$|\psi(t)\rangle = \hat{U}(t_0, t)|\psi(t_0)\rangle. \tag{2.6}$$

By inserting equation (2.6) into the Schrödinger equation (2.1), we obtain a differential equation for the evolution operator:

$$\mathrm{i}\hbar\frac{\partial}{\partial t}\hat{U}(t_0, t)|\psi(t_0)\rangle = \hat{H}(t)\hat{U}(t_0, t)|\psi(t_0)\rangle \tag{2.7}$$

$$\Rightarrow \qquad \mathrm{i}\hbar\frac{\partial}{\partial t}\hat{U}(t_0, t) = \hat{H}(t)\hat{U}(t_0, t) \tag{2.8}$$

For time independent Hamiltonians, the solution is

$$\hat{U}(t_0, t) = \mathrm{e}^{-\mathrm{i}\hat{H}(t-t_0)/\hbar}. \tag{2.9}$$

For closed systems that are described fully quantum mechanically the Hamiltonian is always time independent.

2.1.3 Density Operator

In quantum mechanics, there is the need of describing also mixed states, meaning that a system is in a statistical mixture of different state vectors. This is mostly the case for a subsystem of a bipartite system. In this case, the mixed state does not just express our subjective lack of knowledge, but the fact that the state of the system is unknowable, even if the initial state and the exact Hamiltonian are known.

A simple superposition $|\psi\rangle = \sum_n c_n|u_n\rangle$ of states is not a mixed state, since a linear combination of vectors is just a new vector. Therefore, the operator

$$\hat{\rho} = \sum_i p_i|\psi_i\rangle\langle\psi_i| \qquad \text{with} \sum_i p_i = 1, \tag{2.10}$$

called density operator, is introduced to describe a mixed state. The p_i are the relative weights of the states $|\psi_i\rangle$. The density operator (like any other operator) can be written as a matrix (called density matrix) in the basis $\{|u_n\rangle\}$ with matrix elements

$$(\hat{\rho})_{nk} = \langle u_n|\rho|u_k\rangle. \tag{2.11}$$

The diagonal elements $(\hat{\rho})_{nn}$ are the probabilities of finding the system in state $|u_n\rangle$. There are three important features of the density operator:

1. $\mathrm{Tr}(\hat{\rho}) = 1$,
2. $\hat{\rho}$ is hermitian,

3. $\hat{\rho}$ is positive semidefinite.

The expectation value of an observable for a mixed state is

$$\langle \hat{A} \rangle = \mathrm{Tr}(\hat{A}\hat{\rho}). \tag{2.12}$$

The time evolution of the density operator is obtained by inserting the Schrödinger equation (2.1) into the time-derivative of the density operator (2.10):

$$\frac{\partial}{\partial t}\hat{\rho}(t) = -\frac{\mathrm{i}}{\hbar}[\hat{H}(t), \hat{\rho}(t)]. \tag{2.13}$$

For time independent Hamiltonians one also finds

$$\hat{\rho}(t) = \hat{U}(t)\hat{\rho}(0)\hat{U}^{\dagger}(t). \tag{2.14}$$

An important characteristic quantity of the density operator is the purity

$$P(\hat{\rho}) = \mathrm{Tr}(\hat{\rho}^2), \tag{2.15}$$

with $P \in [\frac{1}{D}, 1]$ where D is the dimension of the Hilbert space. $P = 1$ means that the system is in a pure state, with one of the weights p_i being equal to one and all the others being zero. The maximally mixed state at which all the weights have the same value $p_i = \frac{1}{D}$ has the lowest purity. The purity is invariant under unitary transformations:

$$P(\hat{U}\hat{\rho}\hat{U}^{\dagger}) = P(\hat{\rho}). \tag{2.16}$$

Another quantity we will need is the von Neumann entropy

$$S(\hat{\rho}) = -k_B \mathrm{Tr}\left(\hat{\rho}\ln\hat{\rho}\right), \tag{2.17}$$

where k_B is the Boltzmann constant.

2.1.4 Composed Systems: The Tensor Product

The tensor product is a theoretical tool which allows to construct a composed state space out of different subsystems. For describing the state of two (or more) interacting subsystems, it is not sufficient to consider the two state spaces $\mathcal{H}_1$ and $\mathcal{H}_2$ separately; It is rather necessary to describe the states in the combined state space, which is obtained via the tensor product $\otimes$:

$$\mathcal{H} = \mathcal{H}_1 \otimes \mathcal{H}_2 \tag{2.18}$$

If subsystem 1 is in state $|\phi_1\rangle$ and subsystem 2 in state $|\chi_2\rangle$, then the state of the composed system is

$$|\psi\rangle = |\phi_1\rangle \otimes |\chi_2\rangle = |\phi_1\rangle|\chi_2\rangle. \tag{2.19}$$

This is a so called product state, there is no entanglement between the two subsystems. Interacting systems, though, will generally be entangled. In this case, it is impossible to

determine the state of the composed system based on the local states of the subsystems alone, because these do not contain information about the correlations between the subsystems. For a bipartite system, we can always write

$$\hat{\rho} = \hat{\rho}_1 \otimes \hat{\rho}_2 + \hat{C}_{12}, \tag{2.20}$$

where $\hat{\rho}_1$ and $\hat{\rho}_2$ are the local states of subsystem 1 and 2, and $\hat{C}_{12}$ describes all types of correlations between the two subsystems. Note that $\hat{C}_{12} \neq 0$ does not imply entanglement. The so called reduced states $\hat{\rho}_1$ and $\hat{\rho}_2$ are calculated by

$$\hat{\rho}_1 = \mathrm{Tr}_2(\hat{\rho}) = \sum_{n,n'} \sum_{p} \langle u_n(1) v_p(2) | \hat{\rho} | u_{n'}(1) v_p 2 \rangle \; |u_n(1)\rangle\langle u_{n'}(1)|, \tag{2.21}$$

and analogously for $\hat{\rho}_2$. The $\{|u_n(1)\rangle\}$ are the basis of subsystem 1 and the $\{|v_p(2)\rangle\}$ the basis of subsystem 2.

Also operators have to be defined in the composed state space. An operator $\hat{A}_1$, which by itself only acts on e.g. subsystem 1, can be expanded by the tensor product with the identity operator $\mathbb{1}_2$ acting on subsystem 2:

$$\hat{A}_1' = \hat{A}_1 \otimes \mathbb{1}_2. \tag{2.22}$$

Often, when it is clear on which subsystem an operator acts, the tensor product for e.g. $\otimes\mathbb{1}_2$ is not written explicitly. For the sake of simplicity, I will follow this practice.

2.1.5 Operator Representation

By introducing a set of d^2 orthonormal operators $\hat{Q}_i$ with

$$\mathrm{Tr}\{\hat{Q}_i \hat{Q}_j^\dagger\} = \delta_{ij}, \tag{2.23}$$

any operator $\hat{A}$ acting on a d-dimensional Hilbert space can be represented as

$$\hat{A} = \sum_{i=1}^{d^2} \hat{Q}_i \mathrm{Tr}\{\hat{Q}_i^\dagger \hat{A}\}, \tag{2.24}$$

cf. [28]. Common operator representations are e.g. the transition operators and the Pauli-operators (introduced in the next section).

2.1.6 Two-Level Systems

The simplest, non-trivial quantum system is a two-level system with the two eigenstates $|0\rangle$ and $|1\rangle$ of the Hamiltonian. Naturally, the spin of an electron is such a system (which is therefore often called spin). All operators acting on a two-level system can be represented by four basic matrices, the unit matrix and the three Pauli matrices

$$\hat{\sigma}_x = \begin{pmatrix} 0 & 1 \\ 1 & 0 \end{pmatrix}, \qquad \hat{\sigma}_y = \begin{pmatrix} 0 & -\mathrm{i} \\ \mathrm{i} & 0 \end{pmatrix}, \qquad \hat{\sigma}_z = \begin{pmatrix} 1 & 0 \\ 0 & -1 \end{pmatrix}, \tag{2.25}$$

with

$$[\hat{\sigma}_i, \hat{\sigma}_j] = 2\mathrm{i}\hat{\sigma}_k, \tag{2.26}$$

where $\{i, j, k\}$ is any cyclic permutation of $\{x, y, z\}$. The Hamiltonian of a spin can always be written in the form

$$\hat{H} = \frac{\omega}{2}\hat{\sigma}_z, \tag{2.27}$$

where ω is the energy splitting of the two eigenstates.

Two important operators are the raising and lowering operators

$$\hat{\sigma}_+ = \hat{\sigma}_x + \mathrm{i}\hat{\sigma}_y = |1\rangle\langle 0|, \tag{2.28}$$

$$\hat{\sigma}_- = \hat{\sigma}_x - \mathrm{i}\hat{\sigma}_y = |0\rangle\langle 1|. \tag{2.29}$$

It is always possible to define an inverse temperature (cf. 2.3.3)

$$\beta = \frac{1}{\omega}\ln\frac{\rho_{00}}{\rho_{11}} \tag{2.30}$$

for a two-level system, which is in a mixed state

$$\hat{\rho} = \rho_{00}|0\rangle\langle 0| + \rho_{11}|1\rangle\langle 1|. \tag{2.31}$$

2.1.7 Harmonic Oscillator

The one-dimensional harmonic oscillator describes the dynamics of a particle with mass m confined in a quadratic potential $V(q) = \frac{m\omega^2}{2}q^2$. The Hamiltonian of the system is

$$\hat{H} = \frac{1}{2m}\hat{p}^2 + \frac{m\omega^2}{2}\hat{q}^2. \tag{2.32}$$

We can simplify the Hamiltonian by introducing the so called annihilation and creation operators $\hat{a}$ and $\hat{a}^\dagger$ with

$$\hat{a} = \sqrt{\frac{m\omega}{2\hbar}}\left(\hat{q} + \frac{\mathrm{i}}{m\omega}\hat{p}\right), \tag{2.33}$$

$$\hat{a}^\dagger = \sqrt{\frac{m\omega}{2\hbar}}\left(\hat{q} - \frac{\mathrm{i}}{m\omega}\hat{p}\right), \tag{2.34}$$

so that

$$\hat{H} = \hbar\omega\left(\hat{a}^\dagger\hat{a} + \frac{1}{2}\right) = \hbar\omega\left(\hat{N} + \frac{1}{2}\right) \tag{2.35}$$

with the hermitian operator $\hat{N} = \hat{a}^\dagger\hat{a}$. The commutation relations between the operators $\hat{a}$, $\hat{a}^\dagger$, and $\hat{N}$ are

$$\left[\hat{a}, \hat{a}^\dagger\right] = 1, \tag{2.36}$$

$$\left[\hat{N}, \hat{a}\right] = -\hat{a}, \tag{2.37}$$

$$\left[\hat{N}, \hat{a}^\dagger\right] = \hat{a}^\dagger. \tag{2.38}$$

By denoting the eigenstates and eigenvalues of $\hat{N}$ as

$$\hat{N}|n_i\rangle = n|n_i\rangle \tag{2.39}$$

and using the commutation relations (2.36-2.38), it can be shown that the eigenspectrum of $\hat{N}$ is nondegenerate, that the eigenvalues n are non-negative integers, and that

$$\hat{N}\hat{a}^\dagger|n\rangle = (n+1)\hat{a}^\dagger|n\rangle, \tag{2.40}$$
$$\hat{N}\hat{a}|n \neq 0\rangle = (n-1)\hat{a}|n\rangle. \tag{2.41}$$

Therefore, the eigenenergies of the harmonic oscillator are

$$E_n = \hbar\omega\left(n + \frac{1}{2}\right) \tag{2.42}$$

with $n = 0, 1, 2, \ldots$. The states $|n\rangle$ are called number or Fock states. An important result is that the energy of the groundstate $n = 0$ is not zero.

2.1.8 The Quantum Fidelity

The quantum fidelity is a tool to measure distances of states in Hilbert space. For mixed states, the fidelity is ([22])

$$F(\hat{\rho}_1, \hat{\rho}_2) = \left(\mathrm{Tr}\left\{\left(\sqrt{\hat{\rho}_1}\hat{\rho}_2\sqrt{\hat{\rho}_1}\right)^{\frac{1}{2}}\right\}\right)^2. \tag{2.43}$$

A purification of a mixed state $\hat{\rho}$, which is defined on Hilbert space $\mathcal{H}_\mathrm{A}$, is any pure state $|\Phi\rangle$ in any extended Hilbert space $\mathcal{H}_\mathrm{A} \otimes \mathcal{H}_\mathrm{B}$, for which $\hat{\rho} = \mathrm{Tr}_\mathrm{B}(|\Phi\rangle\langle\Phi|)$. With this definition eq. (2.43) becomes

$$F(\hat{\rho}_1, \hat{\rho}_2) = \max|\langle\Phi_1|\Phi_2\rangle|^2, \tag{2.44}$$

where the maximum is taken over all possible purifications $|\Phi_1\rangle$ and $|\Phi_2\rangle$ (in the same Hilbert space) of $\hat{\rho}_1$ and $\hat{\rho}_2$.

For pure states, the fidelity is

$$F(|\psi_1\rangle, |\psi_2\rangle) = |\langle\psi_1|\psi_2\rangle|^2, \tag{2.45}$$

which only depends on the angle between the two state vectors.

The quantum fidelity has the following properties:

1. $0 \leq F(\hat{\rho}_1, \hat{\rho}_2) \leq 1$, and $F(\hat{\rho}_1, \hat{\rho}_2) = 1$ if and only if $\hat{\rho}_1 = \hat{\rho}_2$.
2. $F(\hat{\rho}_1, \hat{\rho}_2) = F(\hat{\rho}_2, \hat{\rho}_1)$
3. $F(\hat{U}\hat{\rho}_1\hat{U}^\dagger, \hat{U}\hat{\rho}_2\hat{U}^\dagger) = F(\hat{\rho}_1, \hat{\rho}_2)$ for any unitary operator $\hat{U}$.
4. $F(\hat{\rho}, \alpha\hat{\sigma}_1 + (1-\alpha)\hat{\sigma}_2) \geq \alpha F(\hat{\rho}, \hat{\sigma}_1) + (1-\alpha)F(\hat{\rho}, \hat{\sigma}_2), \quad \alpha \in [0, 1]$

2.2 Quantum Optics

Here, we review the concept of field quantization, the quantized atom-field interaction, the laser principle, and some theoretical tools for characterizing the quantum mechanical state of a light field [41, 17, 12].

2.2.1 Quantization of the Free Electromagnetic Field

For quantizing the free electromagnetic field, we start with the classical Maxwell equations (in SI units):

$$\nabla \times \mathbf{B} = \epsilon_0 \mu_0 \frac{\partial \mathbf{E}}{\partial t}, \tag{2.46}$$

$$\nabla \times \mathbf{E} = -\frac{\partial \mathbf{B}}{\partial t}, \tag{2.47}$$

$$\nabla \cdot \mathbf{B} = 0, \tag{2.48}$$

$$\nabla \cdot \mathbf{E} = 0, \tag{2.49}$$

where $\mathbf{E}$, $\mathbf{B}$ are the electric and magnetic field vectors, and ϵ_0 and μ_0 are the free space permittivity and permeability with $(\epsilon_0 \mu_0)^{-\frac{1}{2}} = c$ being the speed of light in vacuum.

Because of (2.47) and (2.48) we can introduce the vector potential $\mathbf{A}$ and the scalar potential Φ satisfying

$$\mathbf{B} = \nabla \times \mathbf{A}, \tag{2.50}$$

$$\mathbf{E} = -\nabla \Phi - \frac{\partial}{\partial t}\mathbf{A}. \tag{2.51}$$

$\mathbf{A}$ and Φ cannot be defined unambiguously, since the gauge transformation

$$\mathbf{A}' = \mathbf{A} - \nabla \chi, \tag{2.52}$$

$$\Phi' = \Phi - \frac{\partial}{\partial t}\chi, \tag{2.53}$$

where χ is an arbitrary scalar field, leaves the physical fields $\mathbf{E}$ and $\mathbf{B}$ invariant. To proceed, we use the Coulomb gauge defined by

$$\nabla \cdot \mathbf{A} = 0, \tag{2.54}$$

leading to

$$\Phi = 0 \tag{2.55}$$

because of (2.49).

Plugging (2.50) and (2.51) into (2.46) yields the wave equation

$$\nabla^2 \mathbf{A} - \frac{1}{c^2}\frac{\partial^2}{(\partial t)^2}\mathbf{A} = 0. \tag{2.56}$$

We now consider the field in a cubic cavity of side length L and volume V with periodic boundary conditions. The general solution of the wave equation (2.56) can be expanded in terms of plane waves

$$\mathbf{A}(\mathbf{r},t) = \sum_{\mathbf{k},s} e_{\mathbf{k},s} \left[A_{\mathbf{k},s} e^{\mathrm{i}(\mathbf{k}\cdot\mathbf{r}-\omega_k t)} + A^*_{\mathbf{k},s} e^{-\mathrm{i}(\mathbf{k}\cdot\mathbf{r}-\omega_k t)} \right] \tag{2.57}$$

where $\mathbf{k}$ is the wave vector of a cavity mode, $s = 1, 2$ is a polarization index, $\mathbf{r}$ is the position, $\omega_k = kc$ (with $k = |\mathbf{k}|$) is the mode frequency, $A_{\mathbf{k},s}$ is a complex amplitude, and $e_{\mathbf{k},s}$ a normalized polarization vector.

The classical Hamilton function of the radiation field is

$$H = \frac{1}{2}\int_V \left(\epsilon_0 \mathbf{E}^2 + \frac{1}{\mu_0}\mathbf{B}^2 \right) dV = 2\epsilon_0 V \sum_{\mathbf{k},s} \omega_k^2 A_{\mathbf{k},s} A^*_{\mathbf{k},s} \tag{2.58}$$

where $\mathbf{B}$ and $\mathbf{E}$ can be obtained from (2.50) and (2.51) using (2.57). By introducing the canonical variables $p_{\mathbf{k},s}$ and $q_{\mathbf{k},s}$ as

$$A_{\mathbf{k},s} = \frac{1}{2\omega_k (\epsilon_0 V)^{\frac{1}{2}}} (\omega_k q_{\mathbf{k},s} + \mathrm{i} p_{\mathbf{k},s}), \tag{2.59}$$

$$A^*_{\mathbf{k},s} = \frac{1}{2\omega_k (\epsilon_0 V)^{\frac{1}{2}}} (\omega_k q_{\mathbf{k},s} - \mathrm{i} p_{\mathbf{k},s}), \tag{2.60}$$

(2.58) becomes a sum over harmonic oscillators of unit mass

$$H = \frac{1}{2}\sum_{\mathbf{k},s} \left(p^2_{\mathbf{k},s} + \omega_k^2 q^2_{\mathbf{k},s} \right). \tag{2.61}$$

We can now quantize the field by replacing the variables $p_{\mathbf{k},s}$ and $q_{\mathbf{k},s}$ with the operators $\hat{p}_{\mathbf{k},s}$ and $\hat{q}_{\mathbf{k},s}$, which allows us to directly apply the results obtained for the harmonic oscillator in Sec. 2.1.7. The Hamilton function (2.58) then becomes the Hamilton operator

$$\hat{H} = \sum_{\mathbf{k},s} \hbar\omega_k \left(\hat{a}^\dagger_{\mathbf{k},s} \hat{a}_{\mathbf{k},s} + \frac{1}{2} \right). \tag{2.62}$$

The quantized energy of the radiation field is

$$E = \sum_{\mathbf{k},s} \hbar\omega_k \left(n_{\mathbf{k},s} + \frac{1}{2} \right), \tag{2.63}$$

where $n_{\mathbf{k},s} = 0,\ 1,\ 2,\ \ldots$ is the excitation number of mode $\mathbf{k}, s$. These excitations are called photons.

The quantized fields have the form

$$\hat{A}(\mathbf{r},t) = \sum_{\mathbf{k},s} \left(\frac{\hbar}{2\omega_k \epsilon_0 V}\right)^{\frac{1}{2}} \mathbf{e}_{\mathbf{k},s} \left[\hat{a}_{\mathbf{k},s} e^{\mathrm{i}(\mathbf{k}\cdot r - \omega_k t)} + \hat{a}^\dagger_{\mathbf{k},s} e^{-\mathrm{i}(\mathbf{k}\cdot r - \omega_k t)}\right], \tag{2.64}$$

$$\hat{E}(\mathbf{r},t) = i \sum_{\mathbf{k},s} \left(\frac{\hbar\omega_k}{2\epsilon_0 V}\right)^{\frac{1}{2}} \mathbf{e}_{\mathbf{k},s} \left[\hat{a}_{\mathbf{k},s} e^{\mathrm{i}(\mathbf{k}\cdot r - \omega_k t)} - \hat{a}^\dagger_{\mathbf{k},s} e^{-\mathrm{i}(\mathbf{k}\cdot r - \omega_k t)}\right], \tag{2.65}$$

$$\hat{B}(\mathbf{r},t) = \frac{1}{c} \sum_{\mathbf{k},s} \frac{1}{k} (\mathbf{k} \times \mathbf{e}_{\mathbf{k},s}) \left(\frac{\hbar\omega_k}{2\epsilon_0 V}\right)^{\frac{1}{2}} \mathbf{e}_{\mathbf{k},s} \left[\hat{a}_{\mathbf{k},s} e^{\mathrm{i}(\mathbf{k}\cdot r - \omega_k t)} - \hat{a}^\dagger_{\mathbf{k},s} e^{-\mathrm{i}(\mathbf{k}\cdot r - \omega_k t)}\right]. \tag{2.66}$$

Note that these field operators are time dependent and are given in the Heisenberg picture.

2.2.2 Atom-Field Interaction

The Hamiltonian of an electron interacting with the electromagnetic field can be derived from a gauge invariance point of view: The value

$$P(\mathbf{r},t) = |\psi(\mathbf{r},t)|^2, \tag{2.67}$$

which gives the probability density of finding the electron at time t at position $\mathbf{r}$, remains unaffected by the transformation

$$\psi'(\mathbf{r},t) = \psi(\mathbf{r},t) e^{\mathrm{i}\chi(\mathbf{r},t)}, \tag{2.68}$$

for an arbitrary choice of $\chi(\mathbf{r},t)$. The Schrödinger equation (2.1), though, is no longer satisfied. The modified Schrödinger equation

$$\left\{-\frac{\hbar^2}{2m}\left[\nabla - \mathrm{i}\frac{e}{\hbar}\mathbf{A}(\mathbf{r},t)\right]^2 + e\Phi(\mathbf{r},t)\right\}\psi(\mathbf{r},t) = \mathrm{i}\hbar\frac{\partial}{\partial t}\psi(\mathbf{r},t), \tag{2.69}$$

is invariant under the transformation (2.68) by setting

$$\mathbf{A}(\mathbf{r},t) \to \mathbf{A}'(\mathbf{r},t) = \mathbf{A}(\mathbf{r},t) + \frac{\hbar}{e}\nabla\chi(\mathbf{r},t), \tag{2.70}$$

$$\Phi(\mathbf{r},t) \to \Phi'(\mathbf{r},t) = \Phi(\mathbf{r},t) - \frac{\hbar}{e}\frac{\partial}{\partial t}\chi(\mathbf{r},t). \tag{2.71}$$

The functions $\mathbf{A}(\mathbf{r},t)$ and $\Phi(\mathbf{r},t)$ are identified as the vector and the scalar potential.

We now consider an electron bound by a potential $V(r)$ to a nucleus located at $\mathbf{r} = 0$ interacting with a plane electromagnetic wave described by $\mathbf{A}(\mathbf{r},t) = \mathbf{A}(t)e^{\mathrm{i}\mathbf{k}\cdot\mathbf{r}}$ in the Coulomb gauge. In the dipole approximation $\mathbf{k}\cdot\mathbf{r} \ll 1$ the vector potential becomes

$$\mathbf{A}(\mathbf{r},t) \approx \mathbf{A}(t). \tag{2.72}$$

We also define a wave function $\phi(\mathbf{r}, t)$ such that

$$\psi(\mathbf{r}, t) = \exp\left[\frac{\mathrm{i}e}{\hbar}\mathbf{A}(t)\cdot\mathbf{r}\right]\phi(\mathbf{r}, t). \tag{2.73}$$

By plugging (2.72) and (2.73) into the Schrödinger equation (2.69) we eventually obtain

$$\mathrm{i}\hbar\frac{\partial}{\partial t}\phi(\mathbf{r}, t) = \left[\frac{1}{2m}p^2 + V(r) - e\mathbf{r}\cdot\mathbf{E}(t)\right]\phi(\mathbf{r}, t) = \left[H_0 - e\mathbf{r}\cdot\mathbf{E}(t)\right]\phi(\mathbf{r}, t), \tag{2.74}$$

where $e\mathbf{r}\cdot\mathbf{E}(t)$ describes the interaction of the atom with the field.

We are going to use the Hamiltonian of (2.74) to describe the dynamics of a two-level atom with energy splitting $\hbar\omega$ and electric dipole moment $\mathbf{d} = e\mathbf{r}$ coupled to one polarized mode of the radiation field $\mathbf{E}$ with frequency ν. The Hamiltonian is

$$\hat{H} = \hat{H}_\mathrm{A} + \hat{H}_\mathrm{F} - \hat{\mathbf{d}}\cdot\hat{\mathbf{E}}, \tag{2.75}$$

where

$$\hat{H}_\mathrm{A} = \frac{1}{2}\hbar\omega\hat{\sigma}_z \tag{2.76}$$

is the energy of the atom, and

$$\hat{H}_\mathrm{F} = \hbar\nu\left(\hat{a}^\dagger\hat{a} + \frac{1}{2}\right) \tag{2.77}$$

is the energy of the radiation field.

The interaction part of the Hamiltonian, $\hat{\mathbf{d}}\cdot\hat{\mathbf{E}}$ can be rewritten using the field operator (2.65) in the Schrödinger picture

$$\hat{\mathbf{E}} = \left(\frac{\hbar\omega_k}{2\epsilon_0 V}\right)^{\frac{1}{2}}\mathbf{e}\left(\hat{a} + \hat{a}^\dagger\right), \tag{2.78}$$

and assuming that the matrix elements of the electric-dipole moment in the basis $|i\rangle$ of the atom are $\langle i|\hat{\mathbf{d}}|j\rangle = \mathbf{d}\,(1 - \delta_{ij})$ so that

$$\hat{\mathbf{d}} = \sum_{i,j}|i\rangle\langle i|\hat{\mathbf{d}}|j\rangle\langle j| = \mathbf{d}\,(\hat{\sigma}_- + \hat{\sigma}_+) \tag{2.79}$$

In the rotating wave approximation ($\hat{\sigma}_-\hat{a} = \hat{\sigma}_+\hat{a}^\dagger = 0$) we obtain

$$\hat{\mathbf{d}}\cdot\hat{\mathbf{E}} = g\left(\hat{\sigma}_-\hat{a}^\dagger + \hat{\sigma}_+\hat{a}\right) = \hat{H}_\mathrm{JC} \tag{2.80}$$

with $g = \left(\frac{\hbar\omega_k}{2\epsilon_0 V}\right)^{\frac{1}{2}}\mathbf{e}\cdot\mathbf{d}$. $\hat{H}_\mathrm{JC}$ is called the Jaynes-Cummings interaction.

2.2.3 Laser Principle

A common laser basically consists of three elements: A gain medium, an energy pump, and a cavity for the radiation field. The energy pump generates a population inversion between two states $|1\rangle$ and $|2\rangle$ with energies E_1 and E_2 (effective two-level atom) of the gain medium, which resonantly interacts with one mode of the cavity field.

There are three possible processes occurring from the interaction of a two-level system with the radiation field: Induced absorption, induced emission and spontaneous emission. The probabilities of these processes to occur are given by the so called rate equations. By comparing these probabilities and considering cavity losses, the attenuation of an electromagnetic wave traveling back and forth a cavity can be derived. The wave is amplified, if the emission of photons into the cavity mode exceeds the absorption plus the cavity losses (threshold condition). This condition typically includes a population inversion between the two levels $|1\rangle$ and $|2\rangle$.

2.2.4 Photon Statistics

By quantizing the radiation field the question arises, which states of the field most closely describe a classical electromagnetic field. Such a classical field may be generated by a classical monochromatic current. The field state, which results from a monochromatic dipole oscillating at some frequency, is a "coherent" state $|\alpha\rangle = e^{\alpha\hat{a}^\dagger - \alpha^*\hat{a}}|0\rangle$, where $\hat{a}^\dagger$ and $\hat{a}$ are the creation and annihilation operator, respectively, and α is a complex parameter. This state turns out to be an eigenstate of the annihilation operator, $\hat{a}|\alpha\rangle = \alpha|\alpha\rangle$, with eigenvalue α. In the Fock representation it is given by

$$|\alpha\rangle = e^{-|\alpha|^2/2} \sum_{n=0}^{\infty} \frac{\alpha^n}{\sqrt{n!}} |n\rangle. \tag{2.81}$$

This state is also called Glauber state. For such a coherent state the uncertainty of the conjugate field variables is minimal and the shape of the corresponding wave function in coordinate representation is invariant during its evolution in a harmonic oscillator potential.

The set of all coherent states $|\alpha\rangle$ is complete:

$$\frac{1}{\pi} \int |\alpha\rangle\langle\alpha| \, \mathrm{d}^2\alpha = 1. \tag{2.82}$$

Two coherent states $|\alpha\rangle$ and $|\alpha'\rangle$ are not orthogonal, i.e.

$$|\langle\alpha|\alpha'\rangle|^2 = e^{-|\alpha-\alpha'|^2}. \tag{2.83}$$

This indicates that the coherent states are overcomplete.

By describing the lasing action fully quantum mechanically (and far above threshold), a Poissonian photon number distribution is obtained, which is also a feature of the coherent state:

$$P(n) = |\langle n|\alpha\rangle|^2 = e^{-\langle\hat{N}\rangle} \frac{\langle\hat{N}\rangle^n}{n!}, \tag{2.84}$$

where $\langle\hat{N}\rangle = |\alpha|^2$.

Second-Order Correlation Function

The photon number distribution of the quantized radiation field depends on the light source, by which the field is generated. Examples are thermal light, coherent light, and single photon states. These different "types" of light can be distinguished by measuring the second-order coherences (e.g. with an Hanbury-Brown-Twiss interferometer). For a single-mode plane-wave field the second-order correlation function is

$$g^{(2)} = \frac{\langle \hat{a}^+ \hat{a}^+ \hat{a}\hat{a} \rangle}{\langle \hat{a}^+ \hat{a} \rangle^2} = 1 + \frac{\langle (\Delta \hat{N})^2 \rangle - \langle \hat{N} \rangle}{\langle \hat{N} \rangle^2}, \tag{2.85}$$

where $\langle (\Delta \hat{N})^2 \rangle = \langle \hat{N} \rangle^2 - \langle \hat{N}^2 \rangle$. For thermal light, which is generated by statistical spontaneous emission, it is $g^{(2)} = 2$, for coherent light, generated by induced emission, it is $g^{(2)} = 1$, and for a single photon state $g^{(2)} = 0$.

Husimi Q Representation

The Husimi Q distribution is a tool to express and represent a quantum state $\hat{\rho}$ in terms of coherent states $|\alpha\rangle\langle\alpha|$. It is defined as

$$Q(\alpha, \alpha^*) = \frac{1}{\pi} \langle \alpha | \hat{\rho} | \alpha \rangle. \tag{2.86}$$

The Q-function is normalized to unity and is proportional to the probability of finding the system in a coherent state $|\alpha\rangle$. Note that the Q-function of a coherent state is not a δ-function, since the coherent states are non-orthogonal.

2.3 Thermodynamics and Statistics

This section is an introduction to the basic concepts of phenomenological thermodynamics and classical thermostatistics [39]. Also the common approach to quantum thermodynamics is given [16].

2.3.1 Phenomenological Thermodynamics

Phenomenological thermodynamics is based on the observation that the state of macroscopically large system is given by very few observables, like e.g. temperature, pressure, volume, etc., called state variables. The state variables of a system remain constant in time after a characteristic relaxation time, if the environment, with which the system interacts, does not change. This state is called equilibrium state. Thermodynamics describes the equilibrium state and transitions between equilibrium states, called processes.

There are two types of state variables:

1. Extensive Variables X, which are proportional to the system size, e.g. total volume.

2. Intensive Variables ξ, which are independent of the system size, e.g. temperature.

These two types of variables form conjugate pairs $\{X_i, \xi_i\}$ (except the internal energy U), and by choosing one variable of each of these pairs (with at least one extensive variable) a complete set of independent state variables can be obtained, defining the thermodynamical state of a system. The other variables are then functions of this set of variables.

Fundamental Laws of Thermodynamics

Thermodynamics is based on four phenomenological laws:

1. *Zeroth law*
   There is an observable called temperature T, which assigns a value to our experience of "hot and cold". Two systems, which are in thermal equilibrium, have the same temperature.

2. *First law*
   During a process, which changes the equilibrium state of the system, the work δW is performed on the system and the heat δQ is transferred. The amount of work performed and heat transferred depends on how the process is realized (δW and δQ are non-integrable), but not the change of the internal energy U, which is given by
   $$\mathrm{d}U = \delta W + \delta Q, \tag{2.87}$$
   since the internal energy is a state variable.

3. *Second law*
   In thermodynamics, there are two types of processes: (i) *Reversible* ones, during which the system is in an equilibrium state virtually at any time, and for which there is a reverse process restoring the initial state of system and environment. (ii) Processes, which cannot be reversed are called *irreversible* and typically describe transitions from non-equilibrium to equilibrium states.

   By introducing the quantity S called entropy, with
   $$\mathrm{d}S = \frac{\delta Q^{\mathrm{rev}}}{T} \tag{2.88}$$
   for reversible processes, one finds that $\mathrm{d}S$ is integrable. For irreversible processes with heat transfer δQ, it is possible to construct a reversible substitute process and observe the quantity
   $$\frac{\delta Q}{T_{\mathrm{ext}}} - \frac{\delta Q^{\mathrm{rev}}}{T} = \frac{\delta Q}{T_{\mathrm{ext}}} - \mathrm{d}S, \tag{2.89}$$
   where T_{ext} is the temperature of the environment providing the heat δQ. The second law of thermodynamics states that
   $$\mathrm{d}S \geq \frac{\delta Q}{T_{\mathrm{ext}}}, \tag{2.90}$$

with the equal sign if and only if the process is reversible.

4. *Third law*
   The third law formulated by Planck says that

$$\lim_{T\to 0} S \to 0. \tag{2.91}$$

   Note that this is not true for systems with a degenerate groundstate.

Fundamental Equation and Thermodynamical Potentials

For reversible processes, the work performed on or by the system is given by

$$\delta W = \sum_i \tilde{\xi}_i \mathrm{d}\tilde{X}_i, \tag{2.92}$$

where the $\{\tilde{\xi}_i, \tilde{X}_i\}$ denote all pairs of conjugate variable except temperature and entropy needed to describe the state of the system. Combining the first (2.87) and the second (2.90) law we obtain the fundamental equation of thermodynamics:

$$\mathrm{d}U = T\mathrm{d}S + \sum_i \tilde{\xi}_i \mathrm{d}\tilde{X}_i. \tag{2.93}$$

If we know the function $U(S, \{\tilde{X}_i\})$, all intensive state variables can be calculated by derivating U with respect to the respective (independent) conjugate extensive variable. U is then called a thermodynamical potential. One could also choose e.g. $\{U, \tilde{X}_i\}$ as independent variables, then the function $S(U, \{\tilde{X}_i\})$ would provide all the information.

If we want to use intensive state variables in the set of independent variables, we can perform a Legendre transformation

$$U(\{X_i\}) \to P(\{\xi_l, X_k\}) = U(\{\xi_l, X_k\}) - \sum_l \xi_l X_l(\xi_l, X_k), \tag{2.94}$$

where $\xi_l = \frac{\partial U}{\partial X_l}$ (while holding constant the other independent variables), and obtain a new potential $P(\{\xi_l, X_k\})$. Replacing all extensive variables with their conjugate intensive ones yields the potential $P(\{\xi_l\}) = 0$, which means that not all independent variables can be intensive.

2.3.2 Classical Thermostatistics

By realizing that any macroscopical system consists of a large number of single particles, which obey the classical equations of motion, the question arises, how the fundamental laws of thermodynamics emerge from classical mechanics. An explanation is based on the *quasi-ergodic hypothesis*, which states that the trajectory of the state $\{q_i, p_i\}$ of a closed system with energy U approaches any point of the hypersurface $H(\{q_i, p_i\}) = U$ in phase space infinitesimally close. Together with the Hamiltonian equations of motion, it follows

that the state along its trajectory remains for the same time in any volume element of equal size. Therefore, the time average of any function $f(\{q_i(t), p_i(t)\})$ is equal to the instantaneous average over all states, which satisfy the given microcanonical conditions:

$$\lim_{T\to\infty} \frac{1}{T}\int_0^T f(\{q_i(t), p_i(t)\})\mathrm{d}t = \frac{1}{\Omega(U)}\int f(\{q_i, p_i\})\delta_{H(\{q_i,p_i\}),U}\Pi_i \mathrm{d}^3q_i\mathrm{d}^3p_i. \tag{2.95}$$

Here $\Omega(U)$ is the volume of the hypersurface $H(\{q_i, p_i\}) = U$. The entirety of all these states with equal statistical weight is called microcanonical ensemble.

Another assumption is *coarse graining*: The phase space is divided into a "coarse" mesh of cells, and it is assumed to be impossible to distinguish two states within the same cell. For chaotic systems, any initial state distribution will spread over the whole hypersurface (but without changing its volume), and with coarse graining it becomes the microcanonical distribution.

Statistical Entropy

Boltzmann postulated, that the entropy S of a closed system is given by

$$S = k_B \ln M, \tag{2.96}$$

where k_B is the Boltzmann constant, and M is the number of microstates satisfying the given microcanonical conditions. By calculating $S(\{X_i\})$ as a function of the extensive variables $\{X_i\}$, all thermodynamical properties of the system are obtained.

A more general definition for systems with macrocanonical conditions is Shannon's entropy and Jaynes' principle

$$S = \mathrm{Max}|_{w_n}\big[-k_B\sum_n w_n \ln w_n\big], \tag{2.97}$$

where w_n is the statistical weight of microstate n. The equilibrium state is obtained by maximizing S with respect to the w_n, and by satisfying $\sum_n w_n = 1$ and the macrocanonical conditions $\sum_n w_n X_{i,n} = \bar{X}_i$ (where $X_{i,n}$ is the value of X_i of the microstate n). This can be done with the method of Lagrange multipliers. Eventually, the result has to be compared to the thermodynamical potentials to identify the Lagrangian multipliers.

One important case is when the system can exchange energy with its environment, which leads to the macrocanical condition $\sum_n w_n E_n = U$, where E_n is the energy of microstate n. Then the w_n are given by

$$w_n = \frac{1}{Z}e^{-\beta E_n}, \tag{2.98}$$

where $\beta = \frac{1}{k_B T}$ is the inverse temperature, and $Z = \sum_n e^{-\beta E_n}$ is the partition function. This is called the canonical state/ensemble.

2.3.3 Quantum Thermodynamics

By explaining how thermostatistics emerges from classical mechanics, one main problem is to explain why there should be a state ensemble, since a classical state is always well defined, even though we may not know it (subjective lack of knowledge). For closed quantum systems, there is a similar problem: a pure state can never relax towards an equilibrium state, because of the unitary dynamics. But by observing only a subsystem of a closed quatum system, the state of the subsystem will generally be a mixed state, even if the total state is pure. Such a mixed state is no consequence of any subjective lack of knowledge, but means that the state of the subsystem is principally unknowable.

Therefore, the common approach is to investigate a bipartite system

$$\hat{H} = \hat{H}_\mathrm{A} + \hat{H}_\mathrm{B} + \hat{H}_\mathrm{AB}, \tag{2.99}$$

where $\hat{H}_\mathrm{A}$ and $\hat{H}_\mathrm{B}$ only act on system A (the system of interest) and B (called environment), respectively, and $\hat{H}_\mathrm{AB}$ is the interaction energy of both subsystems. The state of the total system is generally confined in some subspace of the Hilbert space, because of conservation laws. This subspace is called accessible region. For weak interactions and large environments, it has been shown [16, 19] that the majority of states of the total system yield, by tracing out the environment, nearly the same mixed state for subsystem A, which is the equilibrium state. If a large enough part of the accessible region is reachable for the initial state, then, after a long enough time elapsed, the state of the subsystem will most probably be this equilibrium state, because the velocity of a state in Hilbert space is a constant of motion (for a suitable parameterization).

With energy exchange conditions, the equilibrium state of the small subsystem A is given by the probabilities $P_\mathrm{A}(E_\mathrm{A})$ to find the subsystem in a state with energy E_A:

$$P_\mathrm{A}(E_\mathrm{A}) = g_\mathrm{A}(E_\mathrm{A}) \sum_E \frac{g_\mathrm{B}(E - E_\mathrm{A}) W(E)}{g_\mathrm{tot}(E)}, \tag{2.100}$$

where g_A and g_B are the degeneracy structures of the system and the environment, respectively, E are the possible energies of the total system given by the initial state with probability $W(E)$, and $g_\mathrm{tot}(E)$ is the degeneracy of the combined system for energy E. This equilibrium state depends on the initial state ($W(E)$), but for an exponential degeneracy structure of the environment, $g_\mathrm{B}(E) \propto e^{-\beta E}$, it becomes independent of the initial state. The equilibrium state is then given by

$$P_\mathrm{A}(E_\mathrm{A}) \propto g_\mathrm{A}(E_\mathrm{A}) e^{-\beta E_\mathrm{A}}, \tag{2.101}$$

which is a canonical state with inverse temperature β.

2.4 Gaussian Unitary Ensemble

The theory of random hermitian matrices is important for modeling large, complex systems. The probability density $P(H)$ of the Gaussian unitary ensemble (GUE) is uniquely derived by imposing two requirements [15]:

1. $P(H)$ is invariant with respect to unitary transformations $P(U^\dagger HU) = P(H)$ and
2. The matrix elements of H are statistically independent.

The obtained probability density is

$$P(H) = Ce^{-A\mathrm{Tr}(H^2)}, \tag{2.102}$$

where A is some constant with $A > 0$ and the factor C is for normalization.

For a standard deviation $\sqrt{2}$, the diagonal elements are given by

$$P_\mathrm{d}(H_{ii}) = \frac{1}{2\sqrt{\pi}} e^{-H_{ii}^2/4}, \tag{2.103}$$

and the offdiagonal elements by

$$P_\mathrm{o}(\mathrm{Re}H_{ij}) = \frac{1}{\sqrt{2\pi}} e^{-(\mathrm{Re}H_{ij})^2/2}, \; P_\mathrm{o}(\mathrm{Im}H_{ij}) = \frac{1}{\sqrt{2\pi}} e^{-(\mathrm{Im}H_{ij})^2/2}, \tag{2.104}$$

and $H_{ij} = H_{ji}^*$.

3 The Closed Quantum Mechanical Laser Model

The model presented here is designed to contain the basic elements of a laser: A cavity field mode, a gain medium coupled to the field mode, and an energy pump, which provides energy for the gain medium. We can describe the quantized cavity field mode as a harmonic oscillator. The gain medium is chosen to be a two-level system (spin), and is coupled resonantly to the field mode. The energy pump is formed by a finite number of spins, and interacts with the interfacing spin so that energy can be transferred. If the interfacing spin shows population inversion, we can expect stimulated emission of photons into the field mode.

This model is motivated by the recent interest in light-matter interaction from a thermodynamical point of view, especially the heat engine and heat pump models [5, 47] similar to the three-level maser firstly analyzed as a heat engine by Scovil and Schulz-DuBois [40]. This model consists of a central three-level system with levels $|1\rangle$, $|2\rangle$ and $|3\rangle$, and $E_1 < E_2 < E_3$. The transition $|1\rangle \leftrightarrow |2\rangle$ is coupled to a cold heat bath, and transition $|1\rangle \leftrightarrow |3\rangle$ is coupled to a hot heat bath. The third tansition, $|2\rangle \leftrightarrow |3\rangle$ is coupled to a field mode via the Jaynes-Cummings interaction. By adjusting the energies of the three-level system and the temperatures of the heat baths, the occupation probabilities of the three energy levels can be controlled. This way, it is possible to either get (i) a continuous energy flow into the field mode while energy goes from the hot to the cold heat bath (heat engine), if there is population inversion between $|2\rangle$ and $|3\rangle$, or (ii) an energy flow out of the field mode such that energy goes from the cold to the hot heat bath (heat pump), if there is no population inversion between $|2\rangle$ and $|3\rangle$ and enough energy in the field mode. In [47], the authors claim that the occurring process can essentially be described, from the view of the field mode, as a relaxation process (with heat flow according to LEMBAS (cf. [46] or Sec. 4.1)) of an oscillator coupled to a heat bath with some effective temperature. The partition of this "effective" heat bath into two reservoirs then leads to the heat engine and heat pump operation. We want to analyze such a relaxation process of an oscillator coupled to a (finite) bath modeled by a spin network.

It should be noted that these models have an "internal logic" for the energy exchange between the baths and the field mode, because of the selective coupling of the baths and the field mode to the central three-level system. This "logic" makes them highly non-ergodic: Energy flowing out the hot bath is always divided into two parts, one going into the field mode, and one into the cold heat bath, and vice versa (reverse energy flows). Other processes are not possible. Because of this logic, only a very small subspace of the energy shell in Hilbert space is accessible.

In this chapter, we will discuss the general properties and relaxation dynamics of the model. A detailed analysis of work/heat flows and optical coherences will follow in the next chapter.

3.1 The Model

The schematic structure of the system is shown in Fig. 3.1. The oscillator (with energy splitting ω) is coupled resonantly to spin number 1. This interfacing spin (1) is part of a spin network, which consists of N_S spins with energy splitting ω.

The energy of the spins is ($\hbar = 1$)

$$\hat{H}_\mathrm{S} = \sum_{i=1}^{N_\mathrm{S}} \frac{\omega}{2} \hat{\sigma}_z^{(i)} + \frac{\omega N_\mathrm{S}}{2}, \tag{3.1}$$

where the Pauli matrix $\hat{\sigma}_z^{(i)}$ acts on spin number i, and the second part ($\frac{\omega N_\mathrm{S}}{2}$) is just an energy shift, so that the energy eigenvalues of the spin network are $E_{\mathrm{S},s} = s\omega$ (without interaction), where $s = 0, 1, ..., N_\mathrm{S}$ denotes these eigenenergies . The intercation $\hat{V}_\mathrm{S}$ between the spins will be explained later in detail. The Hamiltonian of the field mode is

$$\hat{H}_\mathrm{F} = \omega \hat{N}, \tag{3.2}$$

where $\hat{N}$ is the occupation number operator. The vacuum energy is set to zero, and the energy eigenvalues are $E_{\mathrm{F},n} = n\omega$, with $n = 0, 1, ...$ denoting these eigenvalues (in the following, we will stick to this denotation of eigenvalues/eigenstates, e.g. s always denotes the eigenvalues of $\hat{H}_\mathrm{S}$ and n always denotes the eigenvalues of $\hat{H}_\mathrm{F}$). Without loss of generality, we set $\omega = 1$. The interaction between spin 1 and the oscillator is the Jaynes-Cummings interaction

$$\hat{V}_\mathrm{JC} = \hat{\sigma}_-^{(1)} \hat{a}^+ + \hat{\sigma}_+^{(1)} \hat{a}, \tag{3.3}$$

where $\hat{\sigma}_-^{(1)}$ and $\hat{\sigma}_+^{(1)}$ are the lowering and raising operators of spin 1, respectively, and $\hat{a}^+$, $\hat{a}$ the creation and annihilation operators of the field mode, respectively.

The total Hamiltonian of the system is

$$\hat{H} = \hat{H}_\mathrm{S} + \hat{H}_\mathrm{F} + a\hat{V}_\mathrm{S} + g\hat{V}_\mathrm{JC} \tag{3.4}$$

where a is the coupling strength between the spins, and g the coupling strength between spin 1 and the field mode. We will only consider the weak coupling limit, i.e. $a, g \ll 1$.

The time evolution of the system is given by

$$\hat{\rho}(t) = e^{-\mathrm{i}\hat{H}t} \hat{\rho}_{(0)} e^{\mathrm{i}\hat{H}t}, \tag{3.5}$$

which is solved numerically by diagonalizing $\hat{H}$.

For the choice of the interaction V_S between the spins we impose the following constraints:

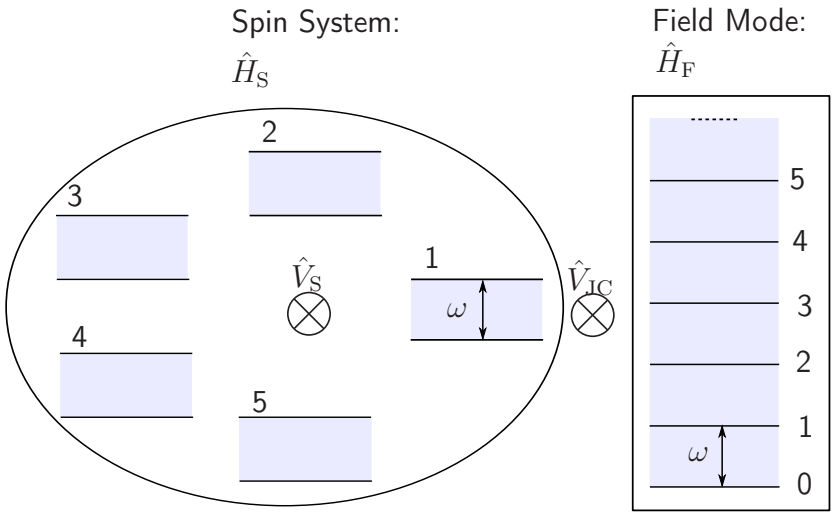

Figure 3.1: Schematic structure of the model (here with $N_S = 6$).

1. The evolution of the total system should be such that a small subsystem (e.g. one spin) relaxes into an equilibrium state, which is approximately the theoretical one (cf. Sec 2.3.3). It is known that for small quantum systems, not all interactions with energy exchange conditions lead to this equilibrium state: In [37, 38], the relaxation behavior of one spin (system) embedded in a spin network (environment), with different forms of structure and interaction, was investigated: The equilibrium state of the spin depends on the details of the interaction between the environmental spins as well as on the details of the interaction between the system spin and the environment. On the other hand, a random interaction matrix from the Gaussian unitary ensemble (GUE) (cf. Sec. 2.4) leads to the theoretical expected equilibrium state [3].

   Therefore, a random matrix from the GUE for the interaction V_S should be a good choice. Then, thermalization within the spin network can be expected, such that all spins have the same equilibrium state, meaning that population inversion of the interfacing spin (1) can be expected, as long as the energy of the spin network is high enough.

2. The second aspect is a numerical one: If $\hat{H}_S + \hat{H}_F$, which is proportional to the number of excited spins plus the number of field excitations ("total excitation number"), is a consevered quantity, the numerical effort can easily and considerably be reduced: In this case, the Hilbert space is divided into the uncoupled eigenspaces of $\hat{H}_S + \hat{H}_F$. By choosing an adequate initial state totally lying within such an eigenspace, all the dynamics will take place in this eigenspace. Then, we only need to consider this eigenspace rather than the total Hilbert space.

The requirements for $\hat{H}_\mathrm{S} + \hat{H}_\mathrm{F}$ being a conserved quantity are

$$\left[\hat{H}_\mathrm{S} + \hat{H}_\mathrm{F}, \hat{V}_\mathrm{JC}\right] = 0, \tag{3.6}$$

$$\left[\hat{H}_\mathrm{F}, \hat{V}_\mathrm{S}\right] = 0, \tag{3.7}$$

$$\left[\hat{H}_\mathrm{S}, \hat{V}_\mathrm{S}\right] = 0. \tag{3.8}$$

The first equation is true for the Jaynes-Cummings interaction with resonant coupling (cf. appendix A). The second one is true because $\hat{V}_\mathrm{S}$ only acts on the spin network. The last equation is true if only states of the spin network with the same eigenenergy $\hat{H}_\mathrm{S}$ can interact, so that $\hat{V}_\mathrm{S}$ becomes block diagonal with each block acting only on an eigenspace of $\hat{H}_\mathrm{S}$:

$$\hat{V}_\mathrm{S} = \sum_s \sum_{i,i'} (\hat{V}_\mathrm{S}^{(s)})_{ii'} |s,i\rangle\langle s,i'| = \begin{pmatrix} \hat{V}_\mathrm{S}^{(1)} & \cdots & 0 \\ & \hat{V}_\mathrm{S}^{(2)} & \\ \vdots & \ddots & \vdots \\ & & \hat{V}_\mathrm{S}^{(s)} \\ 0 & \cdots & \ddots \end{pmatrix}, \tag{3.9}$$

where s denotes the eigenvalues of $\hat{H}_\mathrm{S}$, i and i' the respective eigenstates, and $(\hat{V}_\mathrm{S}^{(s)})_{ii'}$ are the matrix elements of $\hat{V}_\mathrm{S}$. The blocks $\hat{V}_\mathrm{S}^{(s)}$ are then chosen to be random matrices from the GUE as described in point 1.

In this case, the total Hamiltonian is also block diagonal, with each block acting only on one eigenspace of $\hat{H}_\mathrm{S} + \hat{H}_\mathrm{F}$:

$$\hat{H} = \sum_k \sum_{j,j'} (\hat{H}_k)_{jj'} |k,j\rangle\langle k,j'| = \begin{pmatrix} \hat{H}_1 & \cdots & 0 \\ & \hat{H}_2 & \\ \vdots & \ddots & \vdots \\ & & \hat{H}_k \\ 0 & \cdots & \ddots \end{pmatrix}, \tag{3.10}$$

Here k denotes the eigenvalues of $\hat{H}_S + \hat{H}_\mathrm{F}$, j and j' the respective eigenstates, and $(\hat{H}_k)_{jj'}$ the matrix elements of the Hamiltonian. The Hilbert space decomposes into the uncoupled subspaces $\mathcal{H}_k$.

Now we can choose an initial state $\hat{\rho}_0$, which totally lies within such a subspace $\mathcal{H}_k$,

$$\hat{\rho}_0 = \sum_{j,j'} \rho_{k,jj'} |k,j\rangle\langle k,j'|, \tag{3.11}$$

where the $\rho_{k,jj'}$ are matrix elements of the density operator. This way, the numerical effort for calculating the dynamics of the system is considerably reduced, because we only have to consider this subspace $\mathcal{H}_k$.

3. This special choice of $\hat{V}_\mathrm{S}$ has one drawback: There will be only incoherent energy exchange between the field mode and the spin network, if the initial state is of the form (3.11). We can see this, when we calculate the reduced state of the field mode by tracing out the spin network:

$$\hat{\rho}_\mathrm{F} = \sum_{n,n'} \sum_{s,i} \langle n; s, i|\hat{\rho}|n'; s, i\rangle \ |n\rangle\langle n'|, \tag{3.12}$$

where n and n' denote the (nondegenerate) eigenstates of $\hat{H}_\mathrm{F}$, s the eigenvalues of $\hat{H}_\mathrm{S}$ and i the respective eigenstates. Because of the structure of $\hat{V}_\mathrm{S}$, the total state can always be written (using the just introduced notation) as

$$\hat{\rho} = \sum_{n+s=k} \sum_{n'+s'=k} \sum_{i,i'} \rho_{k,ii'} |n; s, i\rangle\langle n'; s', i'|, \tag{3.13}$$

where the first two sums are taken over all n, s, n', s' such that $n + s = n' + s' = k$. Inserting (3.13) into (3.12) yields that $(\hat{\rho}_\mathrm{F})_{nn'}$ is zero if $n \neq n'$, so that $\hat{\rho}_\mathrm{F}$ is diagonal in the Fock representation.

In this chapter, we are only interested in the local energy distribution of the subsystems (e.g. the field mode or one spin). In the next chapter though, we want to discuss coherences within the field mode, which are given by the offdiagonal entries of the reduced density matrix in the energy eigenbasis. Since the special choice of the interaction $\hat{V}_\mathrm{S}$ directly influences these values, we will use a full random matrix from the GUE (full = no special structure).

3.1.1 Parameter

To choose the parameters a and g in (3.4), we first investigate how these parameters influence the equilibrium state of a small subsystem. It has been shown that for small, structured systems the relative coupling strength between different subsystems may affect the equilibrium state of a subsystem [37, 38]. In our model, the Jaynes-Cummings interaction between the field mode and one spin introduces such a structure. To obtain a good choice for the parameters yielding relaxation into the desired equilibrium state, we compare the asymptotical state of the actual dynamics for various values of $\frac{a}{g}$ with the theoretical predictions given in Sec. 3.2.1. By doing so for different numbers N_S of spins in the spin network, we can also estimate whether this effect of the structured interaction depends on the system size, and maybe vanishes in the thermodynamic limit, as could be expected from classical thermodynamics (details of the interaction should not influence the equilibrium state).

For this purpose, we use the initial conditions described in Sec. 3.2 (lasing relaxation: All spins are excited and the field mode is in the ground state), set $g = 0.0001$, and numerically calculate the asymptotical expectation value $\langle\hat{N}\rangle_\mathrm{calc}$ of the photon number. The theoretical value according to (3.23) is $\langle\hat{N}\rangle_\mathrm{theo} = \frac{N_\mathrm{S}}{2}$, where N_S is the number of spins in the spin network. Figure 3.2 shows the ratio $R = \langle\hat{N}\rangle_\mathrm{theo}/\langle\hat{N}\rangle_\mathrm{calc}$ of the theoretical

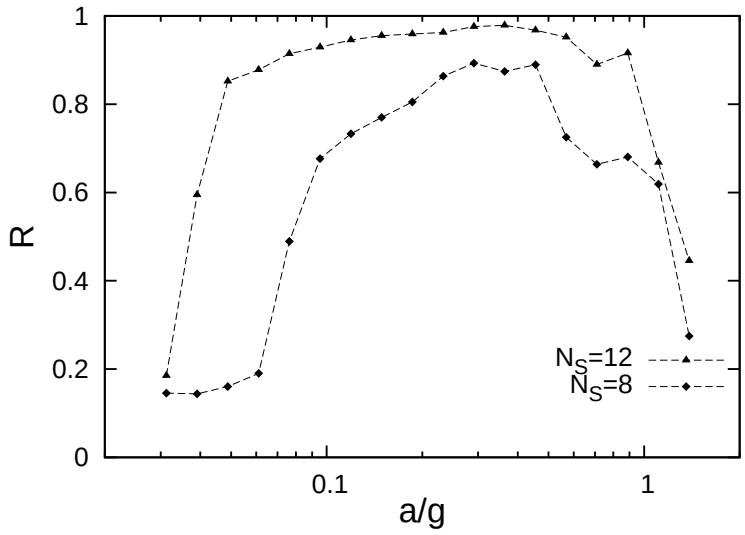

Figure 3.2: Parameter optimization: Dependence of the ratio $R = \langle\hat{N}\rangle_{\text{theo}}/\langle\hat{N}\rangle_{\text{calc}}$ on a/g for different system sizes.

and the actual value, depending on $\frac{a}{g}$ and for $N_{\text{S}} = 8, 12$ spins in the spin network. We can see that for the larger system, the ratio R is closer to the thermodynamical expected value 1 for a wider range of the parameters a and g.

3.1.2 Degeneracy Structure

For calculating the thermodynamically expected equilibrium state (cf. Sec. 2.3.3), we need the degeneracy structure of the subsystems. For the field mode, the degeneracy structure is

$$g_{\text{F}}(n) = 1, \tag{3.14}$$

where n denotes the eigenenergies of the field mode. For one spin, the degeneracy structure is

$$g_{\text{S1}}(m) = 1, \tag{3.15}$$

where S1 means any single spin, and $m = 0, 1$ denotes the eigenenergies of the spin. Because of the weak interaction between the spins, the spin network is a modular system of N_{S} single spins, and the degeneracy structure is a bandstructure with narrow, degenerate energy bands. This degeneracy can be calculated using combinatorics: The degeneracy of the s-th energy band is equal to the number of possibilities to excite s out of N_{S} (numbered and distinguishable) spins:

$$g_{\text{S}}(s) = \binom{N_{\text{S}}}{s}. \tag{3.16}$$

This function is shown in Fig. 3.3 for $N_{\text{S}} = 12$ spins.

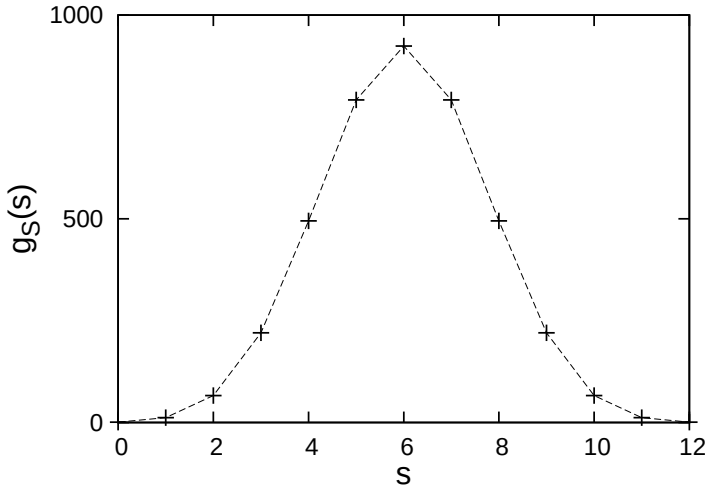

Figure 3.3: Degeneracy structure $g_{\mathrm{S}}(s)$ of a spin network consisting of $N_{\mathrm{S}} = 12$ spins.

3.2 Lasing Relaxation

At first, we will set up the spin network in the highest energy eigenstate, and the field mode in the ground state. Because of the resulting population inversion of the interfacing spin, we expect an energy flow into the field mode with stimulated emission of photons. Though this process should be lasing, the final equilibrium state of the field mode depends on the degeneracy structure of the spin network, and will not necessarily be a (phase-diffused, cf. Sec. 4) Glauber state. However, a laser is far from being in an equilibrium state, but rather a process, which might thermodynamically be interpreted as a steady-state under continuous pumping and loss. We will see that the transient photon number distribution during relaxation is, indeed, nearly Poissonian.

3.2.1 Expected Equilibrium

The thermodynamically expected equilibrium state for a small system A (of interest), which is coupled to a large system B (environment) with energy exchange conditions is given by (2.100):

$$P_{\mathrm{A}}(E_{\mathrm{A}}) = g_{\mathrm{A}}(E_{\mathrm{A}}) \sum_{E} \frac{g_{\mathrm{B}}(E - E_{\mathrm{A}}) W(E)}{g_{\mathrm{tot}}(E)}. \tag{3.17}$$

In the following, we neglect the interaction energies $\hat{V}_{\mathrm{S}}$ and $\hat{V}_{\mathrm{JC}}$, and only consider the energies $\hat{H}_{\mathrm{S}}$ and $\hat{H}_{\mathrm{F}}$. Then, we have $W(E) = \delta_{E_{\mathrm{tot}},E}$, where $E_{\mathrm{tot}} = N_{\mathrm{S}}$ (the number of spins), and discrete systems with $E_{\mathrm{A}} = a$ and $E_{\mathrm{tot}} - E_{\mathrm{A}} = N_{\mathrm{S}} - a = b$, where a and b denote the energy eigenvalues of system A and B, respectively (with energy splitting $\omega = 1$). The expected equilibrium state is

$$P_{\mathrm{A}}(a) = g_{\mathrm{A}}(a) \frac{g_{\mathrm{B}}(N_{\mathrm{S}} - a)}{g_{\mathrm{tot}}(N_{\mathrm{S}})}, \tag{3.18}$$

where again $P_{\mathrm{A}}(a)$ is the probability to find system A in a state with energy $E_{\mathrm{A}} = a$, and g_{A}, g_{B}, and g_{tot} are the degeneracy structures of the system, the environment, and the combined system, respectively.

We consider two (mutually exclusive) perspectives (partitions):

1. System A = one single spin (S1), embedded by B = the other spins and the field mode. Then $g_{\mathrm{A}}(a) = g_{\mathrm{S1}}(m) = 1$ and $m = 0, 1$. For the degeneracy of system B at energy $b = E_{\mathrm{tot}} - m = N_{\mathrm{S}} - m$ we have

$$g_{\mathrm{B}}(N_{\mathrm{S}} - m) = \sum_{s'=0}^{N_{\mathrm{S'}}} \sum_{n=0}^{\infty} \delta_{n+s',N_{\mathrm{S}}-m}\; g_{\mathrm{S'}}(s') g_{\mathrm{F}}(n) = \sum_{s'=0}^{\mathrm{Min}[N_{\mathrm{S'}},N_{\mathrm{S}}-m]} g_{\mathrm{S'}}(s'), \tag{3.19}$$

   where $g_{\mathrm{S'}}(s')$ is the degeneracy of a spin network S' with $N_{\mathrm{S'}} = N_{\mathrm{S}} - 1$ spins and with eigenenergies s'. The term $\delta_{n+s',N_{\mathrm{S}}-m}$ ensures that $E_{\mathrm{tot}} = N_{\mathrm{S}}$. Here we used that $g_{\mathrm{F}}(n) = 1$. The last sum is actually independent of m, because the highest energy band of this spin network is, anyway, $N_{\mathrm{S}} - 1$, so that $g_{\mathrm{S'}}(N_S) = 0$. Inserting (3.19) into (3.18) and using (3.16) we obtain

$$P_{\mathrm{S1}}(m) \propto \sum_{s'=0}^{N_{\mathrm{S'}}} \binom{N_{\mathrm{S'}}}{s'}. \tag{3.20}$$

   In this expected equilibrium state, both eigenstates $m = 0, 1$ have the same occupation probabilities, the energy is $E_{\mathrm{S1}} = 1/2$, and the inversion is $\langle \hat{\sigma}_z \rangle = 0$, which formally yields a local temperature $T = \infty$. Since this consideration applies for any spin, the energy of the total spin network S in equilibrium is expected to be $E_{\mathrm{S}} = N_{\mathrm{S}}/2$.

2. System A = field mode (F), embedded by B, the spin network (S). Here, we have $g_{\mathrm{A}}(a) = g_{\mathrm{F}}(n) = 1$ according to (3.14), and $g_{\mathrm{B}}(b) = g_{\mathrm{S}}(N_{\mathrm{S}} - n) = \binom{N_{\mathrm{S}}}{N_{\mathrm{S}}-n}$ according to (3.16). Using (3.18) we obtain the expected equilibrium photon number distribution

$$P_{\mathrm{F}}(n) = \binom{N_{\mathrm{S}}}{N_{\mathrm{S}} - n}\; g_{\mathrm{tot}}(N_{\mathrm{S}})^{-1}, \tag{3.21}$$

   where the degeneracy of the total system at energy $E_{\mathrm{tot}} = N_{\mathrm{S}}$ is

$$g_{\mathrm{tot}}(N_{\mathrm{S}}) = \sum_{s=0}^{N_{\mathrm{S}}} \sum_{n=0}^{\infty} \delta_{n+s,N_{\mathrm{S}}}\; g_{\mathrm{S}}(s) g_{\mathrm{F}}(n) = \sum_{s=0}^{N_{\mathrm{S}}} \binom{N_{\mathrm{S}}}{s}, \tag{3.22}$$

   analog to (3.19).

   The energy E_{F} of the field mode, which is equal to the expectation value of the photon number $\langle \hat{N} \rangle$, is

$$E_{\mathrm{F}} = \langle \hat{N} \rangle = \sum_n n P_{\mathrm{F}}(n) = \frac{N_{\mathrm{S}}}{2}. \tag{3.23}$$

Figure 3.4 illustrates the "equilibrium state" of the total system, as seen from the respective subsystems, which is basically a microcanonical state of the total system, in which all states with energy E_{tot} have the same occupation probabilities.

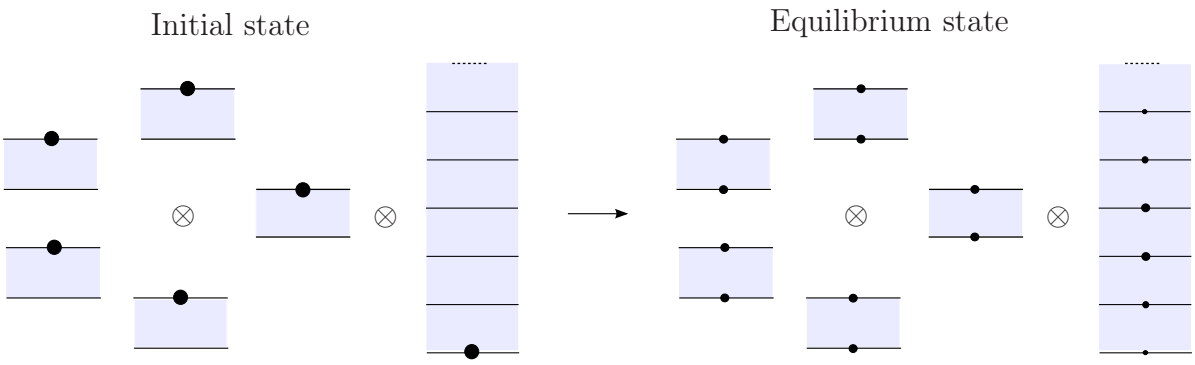

Figure 3.4: Schematic illustration of the initial state and of the equilibrium state.

3.2.2 Dynamics

The simulation of the dynamics of the system is carried out with $N_S = 12$ spins in the spin network. For the field mode, $N_F = 13$ energy levels are taken into account, because the highest excitable state of the field mode is $n = 12$ for the present initial state. The subspace of the Hilbert space, in which all the dynamics takes place, has 4096 dimensions. The coupling strength is set to $g = 0.0001$ and $\alpha = 0.35g$.

Figure 3.5 shows the temporal behavior (a) of the energy of the spin network and (b) of the inversion $\langle \hat{\sigma}_z^{(1)} \rangle$ of spin 1, where the time t is scaled with the coupling strength g. Figure 3.6 shows the dynamics of the field mode: (a) The expectation value $\langle \hat{N} \rangle$ of the photon number, (b) the photon number distribution in equilibrium compared to the expected distribution (the broadening in the numerics is presumably a finite size effect and caused by the structured interaction between the spins and the field mode [37]), (c) the second order correlation function g_2, and (d) the purity $\mathrm{Tr}(\hat{\rho}^2)$. These numerical results show good agreement with the theoretical predictions of the asymptotic equilibrium state as derived in Sec. 3.2.1.

Figure 3.7 shows the Q-Function of the field mode. We can see that the state is phase-diffused, there is no preferred phase for the complex parameter α (all offdiagonal matrix elements of the field mode density matrix in the Fock representation are zero, cf. Sec. 3.1). This feature is a consequence of the special choice of $\hat{V}_S$ and of the initial state.

Finally, in Fig. 3.8 we can see that the transient photon number distribution of the field mode during relaxation is, indeed, nearly Poissonian. These states can thus be described as phase-diffused Glauber states.

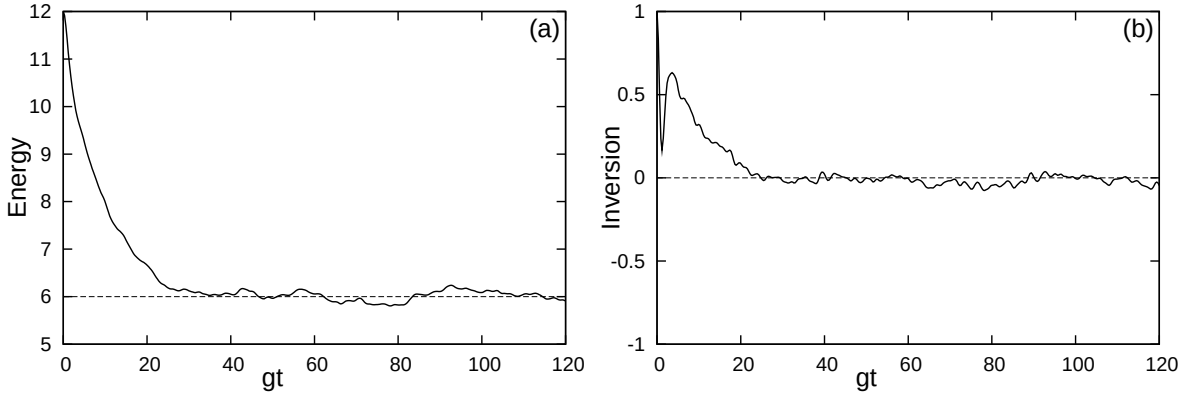

Figure 3.5: Lasing relaxation: (a) Energy in the spin-network, (b) Inversion of spin 1 coupled to the oscillator.

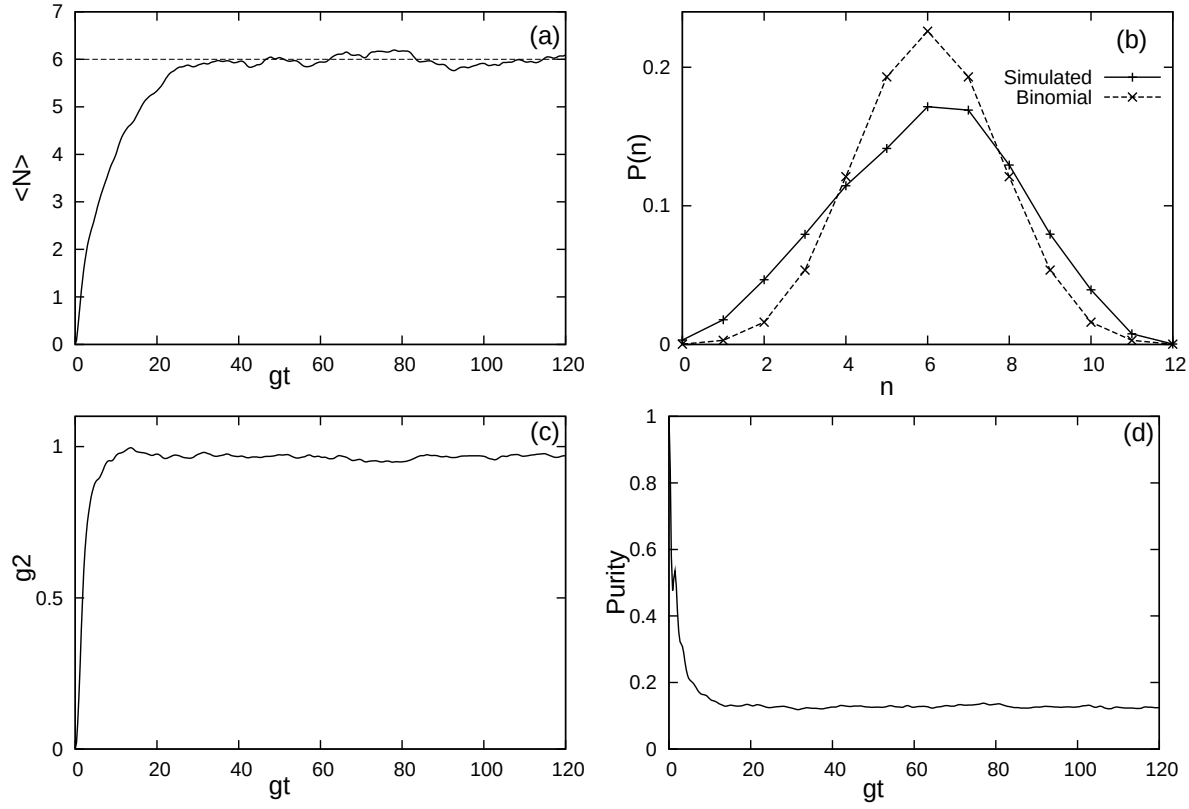

Figure 3.6: Lasing relaxation: (a) expectation value $\langle \hat{N} \rangle$ of the Oscillator, (b) asymptotic photon number distribution $P(n)$, the solid line is the simulated distribution, the dashed line shows the binomial coefficients $\binom{N_S}{n}$ with $N_S = 12$, (c) second-order correlation function, (d) purity of the oscillator state.

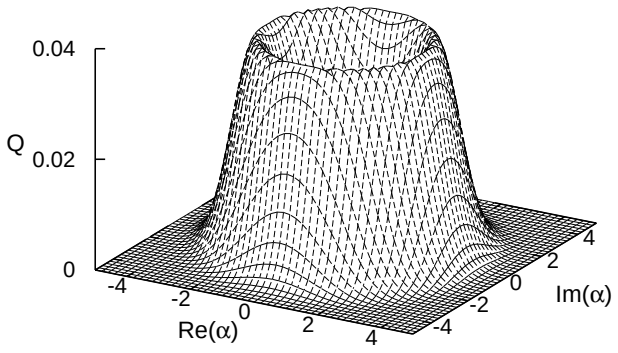

Figure 3.7: Lasing relaxation: Q-Function of the field mode at time $gt = 110$. Parameters are $N_{\mathrm{S}} = 12$, and initial energy in the spin network $E_{\mathrm{S}} = 12$.

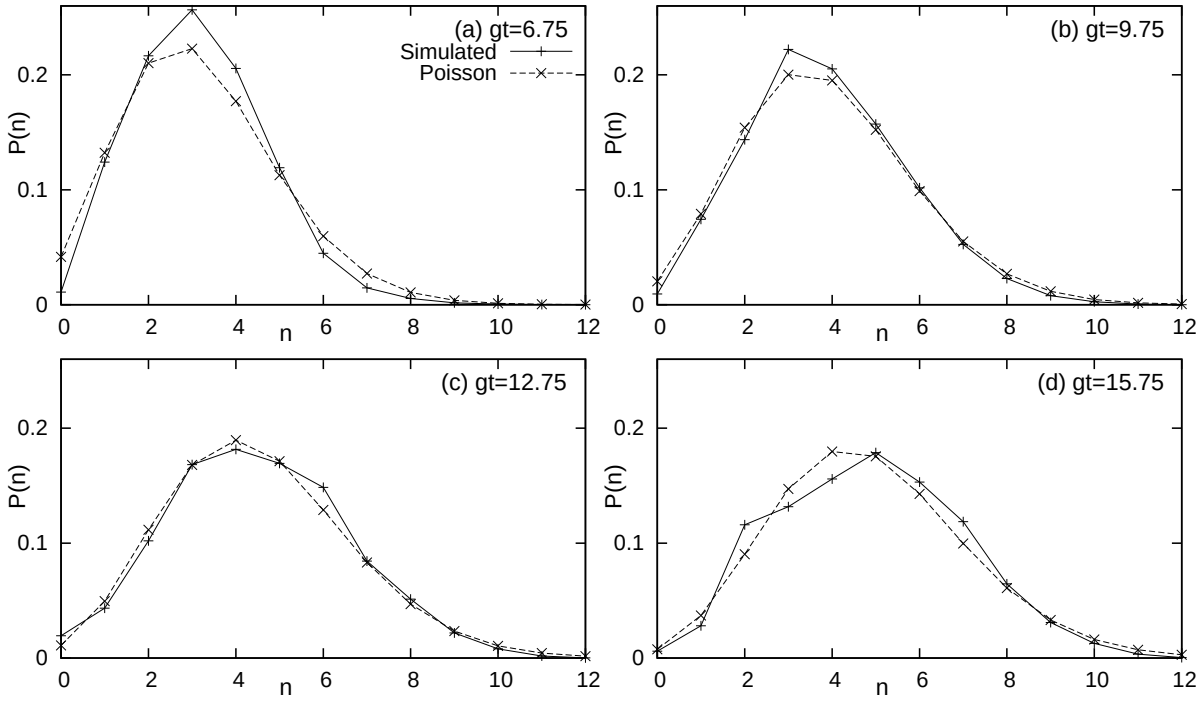

Figure 3.8: Lasing relaxation: Transient photon number distribution (solid line) and Poisson distribution (dashed line) with same $\langle \hat{N} \rangle$ for four sequential times during relaxation.

3.3 Non-Lasing Relaxation

A population inversion of the interfacing spin is not necessary to get an energy flow into the field mode. To show this, we set up the field mode in the ground state (as above), but the spin network in a microcanonical state with $E_{\mathrm{S}} = 6$ and $\langle \hat{\sigma}_z^{(i)} \rangle = 0$ for each spin, so that formally $T = \infty$ for each spin.

Firstly, we calculate the expected equilibrium state of one single spin and of the field mode:

1. System A = one single spin (S1), embedded by B = other spins and the field mode. Analog to Sec. 3.2.1 it is $g_{\mathrm{A}}(a) = g_{\mathrm{S1}}(m) = 1$ and $m = 0, 1$. For the degeneracy of system B at energy $b = E_{\mathrm{tot}} - m = 6 - m$ we now have

$$g_{\mathrm{B}}(6-m) = \sum_{s'=0}^{N_{\mathrm{S'}}} \sum_{n=0}^{\infty} \delta_{n+s',6-m}\; g_{\mathrm{S'}}(s') g_{\mathrm{F}}(n) = \sum_{s'=0}^{6-m} g_{\mathrm{S'}}(s'). \tag{3.24}$$

   The degeneracy of the total system is calculated analogously to (3.22):

$$g_{\mathrm{tot}}(E_{\mathrm{tot}} = 6) = \sum_{s=0}^{6} \binom{N_{\mathrm{S}}}{s}. \tag{3.25}$$

   The occupation probabilities of the single spin are

$$P_{\mathrm{S1}}(m) = \sum_{s'=0}^{6-m} \binom{N_{\mathrm{S'}}}{s'} \; \left(g_{\mathrm{tot}}(6)\right)^{-1}. \tag{3.26}$$

   This state is characterized by $\langle \hat{\sigma}_z \rangle \approx -0.18$.

2. System A = field mode (F), embedded by B, the spin network (S). The derivation is analog to (3.21) and yields

$$P_{\mathrm{F}}(n) = \binom{N_{\mathrm{S}}}{6-n} \; \left(g_{\mathrm{tot}}(6)\right)^{-1}. \tag{3.27}$$

   Here, with $N_{\mathrm{S}} = 12$ the expectation value of the photon number is $\langle \hat{N} \rangle = \sum_n n P_{\mathrm{F}}(n) \approx 1.1$.

We now turn to the simulation results. In Fig. 3.9 we can see that the inversion $\langle \hat{\sigma}_z \rangle$ of the interfacing spin is always below zero. Figure 3.10 shows (a) the expectation value of the photon number $\langle \hat{N} \rangle$ and (b) the asymptotic equilibrium photon number distribution of the field mode. Again, theoretical expectation and simulation are in good agreement.

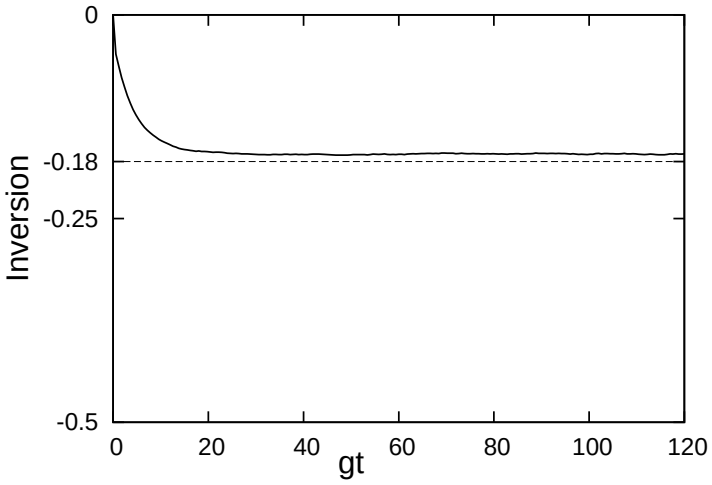

Figure 3.9: Non-lasing relaxation: Inversion $\langle \hat{\sigma}_z \rangle$ of the interfacing spin, the dashed line is the asymptotical expected value.

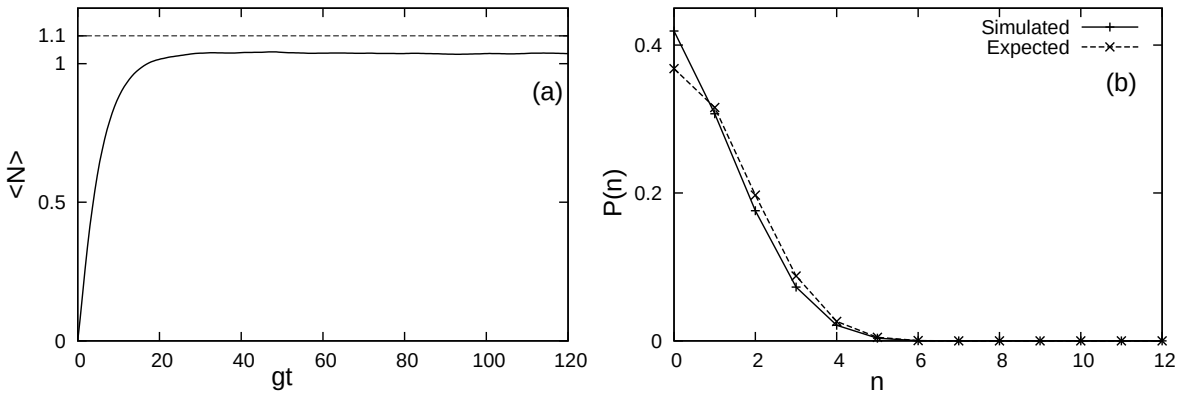

Figure 3.10: Non-lasing relaxation: (a) $\langle \hat{N} \rangle$ of the Oscillator, the dashed line is the asymptotical expected value, (b) photon number distribution $P(n)$ in equilibrium, the solid line is the simulated distribution, and the dashed line the expected distribution (binomial coefficients).

3.4 Discussion

We have seen that the dynamical behavior of our laser model is in accord with the quantum optical expectations as well as with the quantum thermodynamical expectations. Here, the lasing action occurred during the thermodynamical relaxation process. The special choice of the interaction within the energy-pump (spin network) directly led to the phase-diffused optical state. In the next chapter, we will choose a more general Hamiltonian to analyze whether there is typically coherent or incoherent energy flow into the radiation field.

4 Optical Coherences and Heat/Work Analysis

In this chapter, we will further investigate the laser model presented in the previous chapter. These studies will address optical coherences [18] and closely related thermodynamical aspects, namely the heat and work flows from and to the field mode. In view of the three-level maser-like heat engines and pumps [40, 5, 47], we will also discuss to what extend the energy of the radiation field may be "useful".

In 1997, K. Mølmer suggested [30] that the light emitted by typical laser sources should not be in a coherent Glauber state, but in a phase-diffused Glauber state, meaning that all offdiagonal entries of the density matrix (in the Fock representation) are zero, and the diagonal entries are near-Poissonian distributed. In this case, there is no preferred phase for the complex parameter α of the coherent states, and the expectation values of the field amplitude operators vanish. His assumptions are based on an incoherently pumped gain medium. With the same argumentation as in Sec. 3.1, the phase-diffused Glauber state is obtained. He also shows in his work that the results of optical experiments so far only depend on the diagonal matrix elements, i.e. yield the same result for coherent and for phase-diffused Glauber states. In another study by T. Rudolph and B. C. Sanders [35], it is claimed that the state of a single-mode laser output (far above threshold) must be represented by a phase-diffused density matrix, since the phase of the field is unknown. Contrary to this work, K. Nemoto and S. L. Braunstein suggest in [31] that the phase is not just unknown, but rather unobservable, which means that any assumption for the phase (respective any distribution thereof) is equally valid, i.e. also the coherent state.

4.1 LEMBAS Principle

LEMBAS (local effective measurement basis) [46] is a method to systematically investigate the energy change of a system for arbitrary processes, if the dynamics of the system is given (including the effective dynamics induced by the environment). The energy change is split into an effective coherent and an effective incoherent part. The effective coherent part does not alter the local von Neumann entropy, and is therefore assumed to be work. The effective incoherent part, which alters the local von Neumann entropy, is assumed to be heat. Here, I present the important steps we need for calculating these two types of energy change.

To do so, we consider a bipartite system

$$\hat{H} = \hat{H}_{\mathrm{A}} + \hat{H}_{\mathrm{B}} + \hat{H}_{\mathrm{AB}}, \tag{4.1}$$

where $\hat{H}_\mathrm{A}$ and $\hat{H}_\mathrm{B}$ only act on system A (the system of interest) and B ("the rest of the universe"), respectively, and $\hat{H}_\mathrm{AB}$ is the interaction energy of both subsystems. A measurement of the local effective energy of subsystem A then depends on the concrete measuring procedure, introducing a local effective measurement basis.

The state of the total system can be written as

$$\hat{\rho} = \hat{\rho}_\mathrm{A} \otimes \hat{\rho}_\mathrm{B} + \hat{C}_\mathrm{AB}, \tag{4.2}$$

cf. (2.20). The local dynamics of subsystem A is given by

$$\frac{\partial}{\partial t}\hat{\rho}_\mathrm{A} = -\mathrm{i}[\hat{H}_\mathrm{A} + \hat{H}_\mathrm{A}^\mathrm{eff}, \hat{\rho}_\mathrm{A}] + \mathcal{L}_\mathrm{inc}(\hat{\rho}), \tag{4.3}$$

where $\hat{\rho}_\mathrm{A}$ is the reduced state of subsystem A, $\hat{\rho}$ is the state of the total system,

$$\hat{H}_\mathrm{A}^\mathrm{eff} = \mathrm{Tr}_\mathrm{B}\left\{\hat{H}_\mathrm{AB}(\hat{1}_\mathrm{A} \otimes \hat{\rho}_\mathrm{B})\right\} \tag{4.4}$$

is an effective Hamiltonian describing the unitary dynamics induced by B on A, and

$$\mathcal{L}_\mathrm{inc}(\hat{\rho}) = -\mathrm{i}\mathrm{Tr}_\mathrm{B}\left\{[\hat{H}_\mathrm{AB}, \hat{C}_\mathrm{AB}]\right\} \tag{4.5}$$

describes incoherent processes.

By choosing the energy eigenbasis of A as the measurement basis, only parts of $\hat{H}_\mathrm{A}^\mathrm{eff}$ that commute with $\hat{H}_\mathrm{A}$ affect the local effective energy. For a nondegenerate energy eigenbasis $\{|u\rangle\}$ of A this part is given by

$$\hat{H}_1^\mathrm{eff} = \sum_u \langle u|\hat{H}_\mathrm{A}^\mathrm{eff}|u\rangle\, |u\rangle\langle u|, \tag{4.6}$$

with $\hat{H}_\mathrm{A}^\mathrm{eff} = \hat{H}_1^\mathrm{eff} + \hat{H}_2^\mathrm{eff}$ and

$$[\hat{H}_\mathrm{A}^\mathrm{eff}, \hat{H}_1^\mathrm{eff}] = 0, \tag{4.7}$$
$$[\hat{H}_\mathrm{A}^\mathrm{eff}, \hat{H}_2^\mathrm{eff}] \neq 0, \tag{4.8}$$

if $\hat{H}_2^\mathrm{eff} \neq 0$.

The corresponding operator for an energy measurement in the energy eigenbasis of $\hat{H}_\mathrm{A}$ is

$$\hat{H}'_\mathrm{A} = \hat{H}_\mathrm{A} + \hat{H}_1^\mathrm{eff} \tag{4.9}$$

Using (4.3) and assuming $\hat{H}_\mathrm{A}$ to be time independent, we obtain a formula for calculating the effective internal energy change of A:

$$\begin{aligned}\mathrm{d}U_\mathrm{A} &= \frac{\mathrm{d}}{\mathrm{d}t}\mathrm{Tr}\left\{\hat{H}'_\mathrm{A}\hat{\rho}_\mathrm{A}\right\}\mathrm{d}t = \mathrm{Tr}\left\{\dot{\hat{H}}'_\mathrm{A}\hat{\rho}_\mathrm{A} + \hat{H}'_\mathrm{A}\dot{\hat{\rho}}_\mathrm{A}\right\}\mathrm{d}t \\ &= \mathrm{Tr}\left\{\dot{\hat{H}}_1^\mathrm{eff}\hat{\rho}_\mathrm{A} - \mathrm{i}[\hat{H}'_\mathrm{A}, \hat{H}_2^\mathrm{eff}]\hat{\rho}_\mathrm{A} + \hat{H}'_\mathrm{A}\mathcal{L}_\mathrm{inc}(\hat{\rho})\right\}\mathrm{d}t.\end{aligned} \tag{4.10}$$

By observing that the first two terms induce unitary dynamics on A, and that only the last term changes the local von Neumann entropy, we define

$$\delta W_{\mathrm{A}} = \mathrm{Tr}\left\{\dot{\hat{H}}_1^{\mathrm{eff}}\hat{\rho}_{\mathrm{A}} - \mathrm{i}[\hat{H}'_{\mathrm{A}}, \hat{H}_2^{\mathrm{eff}}]\hat{\rho}_{\mathrm{A}}\right\}\mathrm{d}t, \tag{4.11}$$

$$\delta Q_{\mathrm{A}} = \mathrm{Tr}\left\{\hat{H}'_{\mathrm{A}}\mathcal{L}_{\mathrm{inc}}(\hat{\rho})\right\}\mathrm{d}t. \tag{4.12}$$

Using these formulas, any local energy change can be systematically split into heat and work.

4.2 Lasing Relaxation

As discussed in Sec. 3.1, we choose the interaction $\hat{V}_{\mathrm{S}}$ between the spins to be a random matrix from the GUE with no particular structure. We use the same initial state as in Sec. 3.2 (all spins are excited and the field mode is in the ground state), and expect lasing action during relaxation. This time though, we cannot expect the optical coherences to vanish as a consequence of the structure of $\hat{V}_{\mathrm{S}}$: Coherent energy change of the field mode is in principle possible. The numerical calculations are now carried out with $N_{\mathrm{S}} = 8$ spins only and $N_{\mathrm{F}} = 10$ levels of the field mode taken into account (because $[\hat{H}_{\mathrm{S}} + \hat{H}_{\mathrm{F}}, \hat{V}_{\mathrm{S}}] \neq 0$, more than 8 photons may be excited in the field).

For investigating the optical coherences we calculate the Husimi Q-function (2.86), and the field purity

$$P = \mathrm{Tr}(\hat{\rho}_{\mathrm{F}}^2) \tag{4.13}$$

compared to the purity of the diagonal part

$$\hat{\rho}_{\mathrm{F}}^{\mathrm{diag}} = \sum_n (\hat{\rho}_{\mathrm{F}})_{nn}|n\rangle\langle n|. \tag{4.14}$$

The work/heat analysis is done with LEMBAS. The local measurement basis is the energy eigenbasis of $\hat{H}_{\mathrm{F}}$. These two questions are closely related, since coherent/incoherent effective energy changes in this basis are identified as work/heat by LEMBAS.

Figure 4.1 (a) shows the asymptotic Q-function of the field mode and (b) the purity of the field mode. Both graphs indicate that the field is in a phase-diffused state without optical coherences. This is in accord with the work/heat analysis using LEMBAS. Figure 4.2 shows the energy gain of the field mode compared to the accumulated heat flow: The transferred energy is heat only.

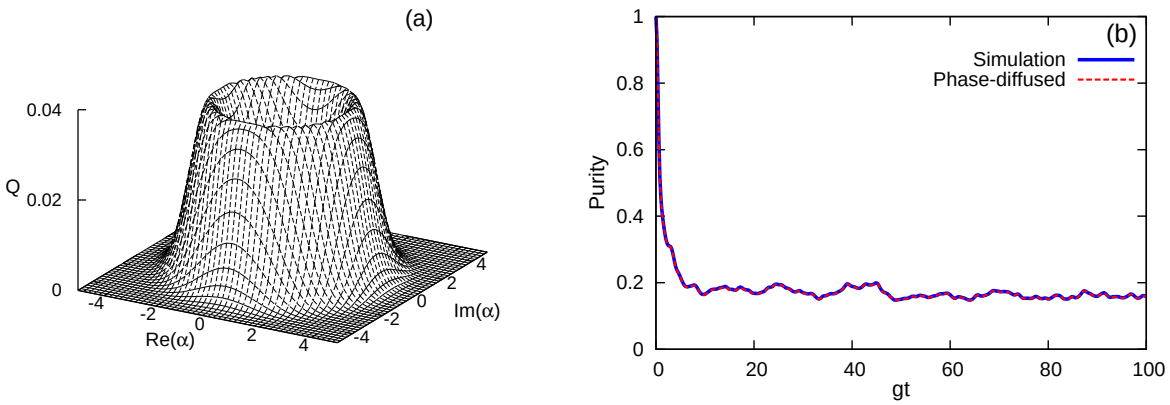

Figure 4.1: Lasing relaxation: (a) Q-function of the field mode at time $gt = 90$, (b) purity of the field, the solid line is the result of the simulation, and the dashed line the purity of the same photon number distribution, but with all offdiagonal elements of the density matrix set to zero. Parameters are $N_{\mathrm{S}} = 8$, and initial energy in the spin network $E_{\mathrm{S}} = 8$.

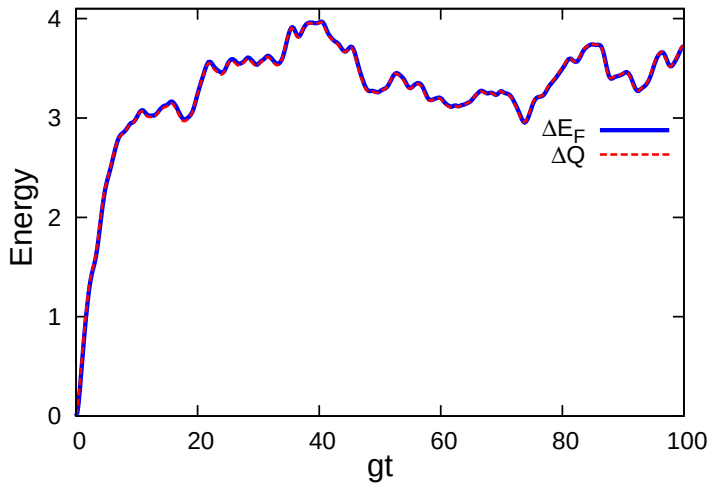

Figure 4.2: Lasing relaxation: Energy change ΔE_{F} and accumulated heat flow ΔQ of the field mode. Here, $\Delta E_{\mathrm{F}} = \Delta Q$.

4.3 Energy Flow into the Spin Network

Here we investigate the "inverse" energy flow from the initial excited field mode into the spin network. We consider an initial state with the spin network ($N_S = 8$) being in its ground state and the field mode being in a state with $\langle \hat{N} \rangle = 4$. For this given $\langle \hat{N} \rangle$ two different states will be compared: (i) A phase-diffused Glauber state, (ii) a coherent Glauber state. The thermodynamical expected equilibrium state of a small subsystem is the same for both initial states: Generally, the equilibrium state of a small subsystem A of a bipartite system $A + B$ with energy exchange conditions depends on the initial state, but only on the initial energy probability distribution $W(E)$ of the total system (cf. Sec. 2.3.3):

$$P_A(E_A) = g_A(E_A) \sum_E \frac{g_B(E - E_A)W(E)}{g_{tot}(E)}. \tag{4.15}$$

Figure 4.3 shows the change of the field energy ΔE_F as a function of time together with the LEMBAS analysis of this ΔE_F for (a) an initial phase-diffused Glauber state of the field mode, and (b) an initial coherent Glauber state: The evolution of ΔE_F is the same. However, for the coherent Glauber state the dominating energy contribution is work, $|\Delta W| > |\Delta Q|$, as might have been expected, while for the phase-diffused Glauber state $\Delta E = \Delta Q$. So, for comparing these two processes, the separation of the energy exchange into heat and work seems to be of limited value: The redistribution of energy is the same.

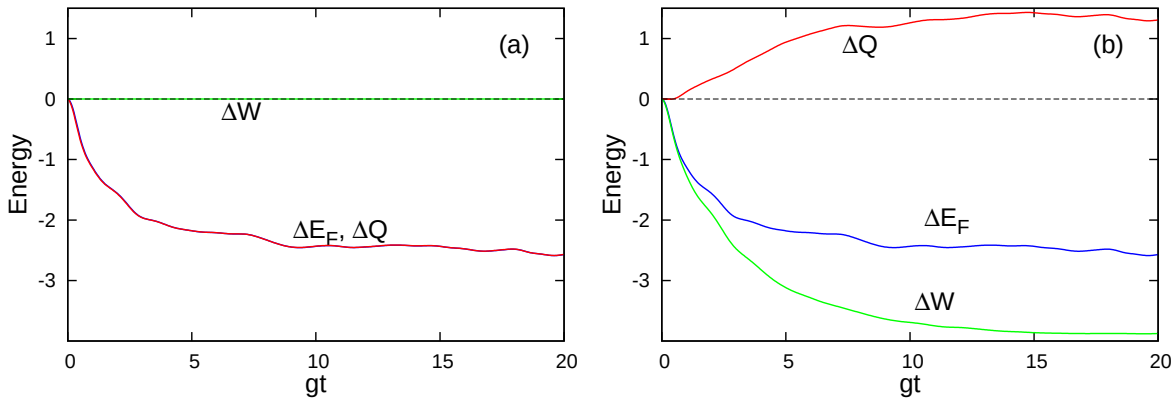

Figure 4.3: Inverse energy flow: Energy change ΔE_F of the field mode and accumulated heat and work flows for (a) initial phase-diffused Glauber state, where $\Delta E_F = \Delta Q$, and (b) initial coherent Glauber state. Note the opposite sign of ΔQ.

4.4 "Usefulness" of the Field Energy

We will see that from a thermodynamical point of view, namely the principle of the increase of entropy (second law), the energy in the field mode obtained during lasing relaxation might, to some extent, be directly used to perform work on another system. This is mainly an effect of the local negative temperature (population inversion) of the interfacing spin, which is necessary to get lasing action.

4.4.1 Negative Temperatures and the Second Law

The temperature of a system in thermal equilibrium can be calculated by

$$T^{-1} = \left(\frac{\partial S}{\partial U}\right)_X, \tag{4.16}$$

while holding constant all other independent variables X, which appear in the fundamental equation. If the slope of the entropy S as a function of the internal energy U becomes negative, the temperature also does. This condition is given by e.g. spin systems, which have an upper bound for the internal energy. Figure 4.4 shows qualitatively the entropy of a spin network. The mirror symmetry (to U_0) of the graph is also referred to as "thermal duality" [36]. For $U > U_0$, the temperature would be negative (if the state is canonical), respectively the spin network would impart a negative temperature on another spin, which is the case in our model during the lasing relaxation. Negative temperatures are actually hotter than positive temperatures: (i) the internal energy of a system is higher for negative temperatures than for positive temperatures, and (ii) by connecting two heat baths, one with a negative temperature and the other with a positive temperature, heat flows form the former to the latter one. By introducing the negative inverse temperature $T' = -\beta$ the algebraic order $T'_{\text{hot}} > T'_{\text{cold}}$ and the "physical" order from hot to cold would coincide [34]: $T' : -\infty \cdots 0 \cdots \infty$ monotonous (cf. Fig. 4.4), contrary to the convential temperature T: $+0 \cdots \pm\infty \cdots -0$.

On the basis of the increase of entropy, the possible effects of thermodynamic machines operating with heat baths at negative temperatures can be derived [23]. There, heat engines and heat pumps are defined by the energy change of the work reservoir: If there is an energy flow into the work reservoir, this is a heat engine, and vice versa for heat pumps (defining the heat pump by an energy flow from the cold to the hot reservoir, and vice versa for the heat engine, would yield negative efficiencies). Using these definitions, analogies between heat engines at positive (negative) temperatures and heat pumps at negative (positive) temperatures can be found:

1. For heat engines at negative temperatures, in the ideal reversible case (process with $\delta S = 0$) heat flows from the cold ($-\beta_{\text{c}} = T'_{\text{c}}$) to the hot ($-\beta_{\text{h}} = T'_{\text{h}} > T'_{\text{c}}$) bath, just like for heat pumps at positive temperatures (though with an inverse sign for the work flow). It is always possible to extract heat from one bath with no other effect than performing the same amount of work. This is analog to heat baths at positive temperatures, but with inverse energy flows: Here, converting work into heat is always possible.

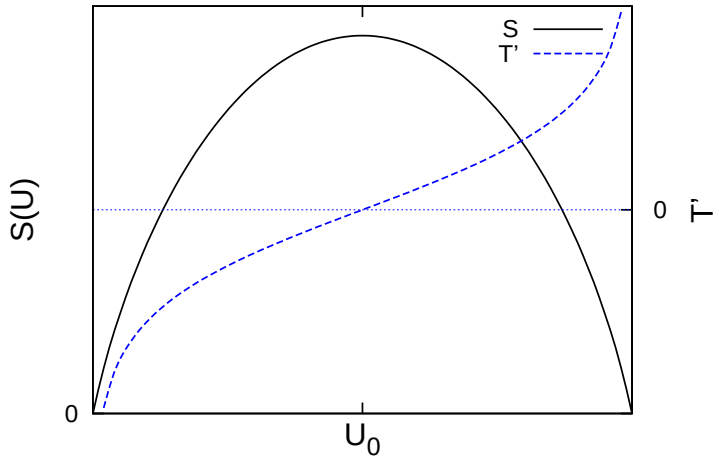

Figure 4.4: Qualitative graph of the entropy S and the negative inverse temperature T' for a spin network as a function of the internal energy U (of the energy bands).

2. For heat pumps at negative temperatures, there is a heat flow from the hot to the cold reservoir, just as in the case of a heat engine at positive temperatures (again with an inverse sign for the work flow).

All these effects can be explained by the negative slope of the function $S(U)$, e.g. extracting energy from a heat bath with negative temperature leads to a local increase of entropy, and using this energy with no other effect than performing the same amount of work on another system is in accord with the second law. (A similar argument is used in [13], where the authors claim that a heat bath at $T = \infty$ becomes a repository for work. In this limit, the slope of the entropy function $S(U)$ is zero, and removing energy from the heat bath does not change the entropy)

4.4.2 Field Energy

This argument (based on the principle of the increase of entropy) can also be applied to the phase-diffused Glauber state of the field mode obtained during lasing action, e.g. like in our model: It should now be possible to extract energy from the field without decreasing its von Neumann entropy – $\Rightarrow \delta S_{\mathrm{F}} \geq 0$ while $\delta E_{\mathrm{F}} < 0$ –, as long as the state of the field is not the one with the highest entropy for the given microcanonical conditions (the internal energy in this case). According to the second law, it may therefore be possible to use this energy to perform work on another system.

Of course, not all of the energy stored in such a field can be used this way, since the entropy of the ground state is zero. The lowest (in terms of internal energy), by energy extraction reachable state without decreasing the local von Neumann entropy is a thermal state with the same entropy as the initial state (e.g. the phase-diffused

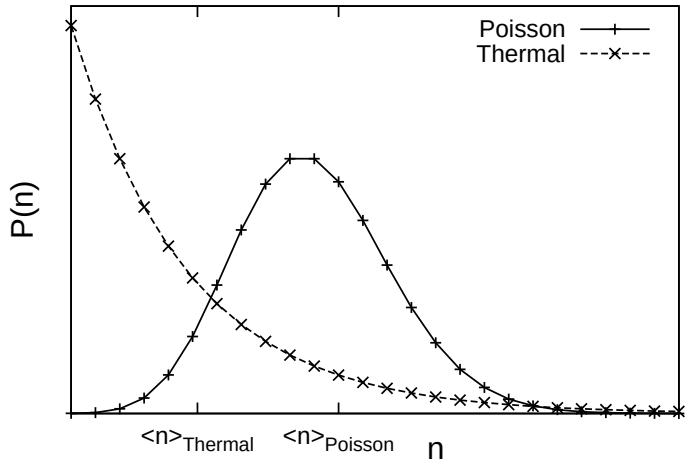

Figure 4.5: Poissonian and thermal photon number distribution with the same von Neumann entropy.

Glauber state). Therefore, the amount of energy extractable from the field mode without decreasing the local von Neumann entropy can be determined by calculating the energy of a thermal distribution with the same entropy as the initial distribution, and comparing the energies of both distributions (cf. App. B). Fig. 4.5 shows a Poissonian photon number distribution, cf. (2.84), with a mean photon number $\langle \hat{N} \rangle = 10$ and a thermal photon number distribution, cf. (2.101), with the same von Neumann entropy (in this case $\beta \approx 0.21/\hbar\omega$). One can clearly see the energy difference of these two distributions. An arising question is how this energy difference depends on the mean photon number of the Poisson distribution. Fig. 4.6 shows this dependence of the energy ration

$$P = \frac{E_{\mathrm{P}} - E_{\mathrm{th}}}{E_{\mathrm{P}}} = \frac{\hbar\omega\langle \hat{N} \rangle - E_{\mathrm{th}}}{\hbar\omega\langle \hat{N} \rangle}, \tag{4.17}$$

where $E_{\mathrm{P}} = \hbar\omega\langle \hat{N} \rangle$ is the energy of the Poisson distribution for an oscillator with mean photon number $\langle \hat{N} \rangle$ and energy splitting $\hbar\omega$, and E_{th} is the energy of a thermal distribution with the same entropy. For $\langle \hat{N} \rangle \to \infty$, we get $P \to 1$, which means that nearly all the internal energy of this field could be used to perform work (since P cannot be calculated analytically, no limits can be obtained, cf. B).

Under isentropical conditions, one would thus expect a crucial difference between the coherent Glauber state and the phase-diffused Glauber state, because in the former case the local von Neumann entropy is zero, and therefore all the energy stored in the field could be used to perform work. But this is not the case: A thermodynamical relaxation with energy exchange conditions must yield the same equilibrium state for both initial states, and this is what actually happens in our model (cf. Sec. 4.3). In fact, during the relaxation process, the local entropy of the field mode changes (cf. Fig. 4.7).

These considerations also do not apply to the three-level maser models discussed in Sec. 3. In [47] it has been shown that even if the field mode is initially in a thermal

state, the heat pump scenario may be realized. The possibility of using heat to operate a heat pump (energy flow from the cold to the hot bath) in this model seems to be an effect of the "inner logic" caused by the selective coupling (interaction) of the baths and the field mode to the central three-level system (this heat pump scenario is only possible, if the energy (temperature) of the field mode is high enough, such that there is no contradiction to the second law).

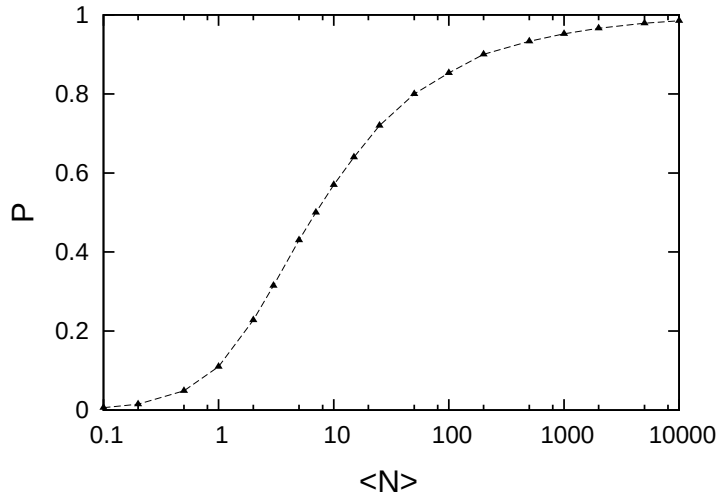

Figure 4.6: Energy ratio $P = \frac{\hbar\omega\langle\hat{N}\rangle - E_{\mathrm{th}}}{\hbar\omega\langle\hat{N}\rangle}$ of the Poissonian and of the thermal distribution with same entropy.

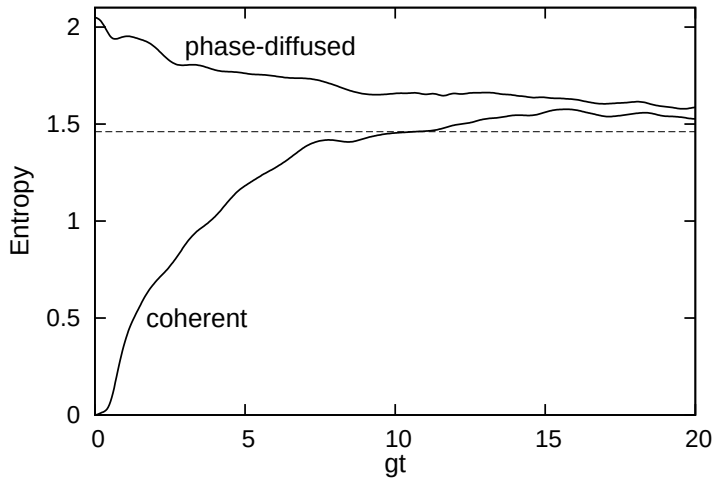

Figure 4.7: Inverse energy flow: Entropy (qualitative) of the field mode for the two initial states (phase-diffused and coherent Glauber state). The dashed line is the expected equilibrium entropy, the deviation is a finite-size effect.

5 Emergence of Irreversibility in Quantum Systems

In the proceeding chapters the emergence of thermodynamic properties in closed quantum-optical scenarios has been demonstrated. We focused on "apparent" relaxation behavior of quantum subsystems embedded in larger quantum environments. This relaxation can be viewed as a signature of the second law.

There has been a long-standing debate about the significance of the second law for the appearance of an arrow of time. One main observation of thermodynamics clearly is the irreversibility of a process [6, 27], which is associated with entropy production. It includes, one the one hand, the relaxation into equilibrium (as discussed in chapters 3 and 4), but on the other hand, also the impossibility to return to the initial state. As will be shown now, both these aspects require separate attention. The impossibility to return is in stark contrast to the underlying microscopic dynamics, which are invariant in time (in quantum mechanics as well as in classical mechanics). This contradiction is addressed by the so called Loschmidt echo: In principle, one could reverse all velocities of a (classical) gas to get back to the initial state [25]. In fact, the only argument to solve this paradox seems to be operational, namely limited control over the system.

Limited control can be modeled in various ways: The Loschmidt reversal (echo) does not work, e.g., in chaotic systems, because any error of the initial state in phase space would grow exponentially in time, and we assume that it is not possible to set up the system in a state with arbitrary accuracy. In quantum mechanics, however, this argument does not hold anymore: An error of the initial state, measured by the quantum fidelity (cf. Sec. 2.1.8), does not change in time, because the fidelity is invariant under unitary transformations.

For controlling the state of a quantum system, such that it evolves back into the initial state, we would need to somehow control the Hamiltonian. This is what is done in various spin-echo experiments, where a series of RF-pulses is applied on a spin system, effectively changing the Hamiltonian such that an echo can be measured [21] (of course, such experiments are generally very difficult to realize). Other examples of dynamical control is quantum information processing, where external fields are used for controlling the Hamiltonian [9], and the wave-front reversal in nonlinear optics [29]. Despite these rather special scenarios one may argue that any system could, in principle, be subject to some kind of echo testing [45].

In the following we assume that our actual control over the Hamiltonian is limited, thereby introducing some error. Another problem for any "real" experiment would be that a system cannot be perfectly isolated from its environment, generating further perturbations [32]. The stability (or better to say the instability) of the system with

respect to any such perturbations of the Hamiltonian may thus be seen as an important source of irreversibility. We will consider systems subject to unitary dynamics only, which may be classified as closed in the sense that there are no incoherent dynamics, even though we influence the system from the "outside".

5.1 Loschmidt Echo in Quantum Systems

An easy way to (numerically) model the quantum Loschmidt echo for general systems is the following: We start in an initial state α, and let the system evolve during time τ under the Hamiltonian $\hat{H}$ into state β. After time τ, we change the sign of the Hamiltonian, effectively reversing the dynamics, and introduce the error $\epsilon\hat{V}$ because of our limited control:

$$-\hat{H}' = -\hat{H} - \epsilon\hat{V}, \tag{5.1}$$

where the parameter ϵ controls the strength, $\hat{V}$ the type of perturbation. After a second time period τ we reach state α', and the fidelity between state α and α' tells us the probability of measuring the state α and α' to be the same, *i.e.* the probability of success. There are obviously initial states to be excluded, like eigenstates or oscillating states. This can be ensured by postulating a time scale τ_{dyn} on which

$$F(\psi_\alpha, \psi_\beta(\tau > \tau_0)) \to 0 \;\Leftrightarrow\; \tau_0 > \tau_{\text{dyn}}. \tag{5.2}$$

Because of the unitarity of the dynamics, the result of the fidelity measurement is kind of independent of the "direction" of the procedure. Figure 5.1 shows a schematic illustration of the state evolution in Hilbert space subject to different Hamiltonians. Mathematically, the fidelity between states α and α' and between states β and β' is just the same: The four states are connected in the following way ($\hbar = 1$):

$$\begin{aligned}
|\psi_{\alpha'}\rangle &= e^{\mathrm{i}\hat{H}'\tau} e^{-\mathrm{i}\hat{H}\tau} |\psi_\alpha\rangle, \\
|\psi_\beta\rangle &= e^{-\mathrm{i}\hat{H}\tau} |\psi_\alpha\rangle, \\
|\psi_{\beta'}\rangle &= e^{-\mathrm{i}\hat{H}'\tau} |\psi_\alpha\rangle.
\end{aligned}$$

Therefore, the fidelities are

$$\begin{aligned}
F(\psi_\alpha, \psi_{\alpha'}) &= |\langle\psi_\alpha|\psi_{\alpha'}\rangle|^2 \\
&= |\langle\psi_\alpha| e^{\mathrm{i}\hat{H}'\tau} e^{-\mathrm{i}\hat{H}\tau} |\psi_\alpha\rangle|^2 \\
&= |\langle\psi_{\beta'}|\psi_\beta\rangle|^2 = F(\psi_\beta, \psi_{\beta'}).
\end{aligned} \tag{5.3}$$

This relation also holds for mixed states (cf. Sec. 2.1.8):

$$F(\hat{U}'\hat{\rho}_\alpha\hat{U}'^\dagger, \hat{U}'\hat{\rho}_{\alpha'}\hat{U}'^\dagger) = F(\hat{\rho}_\beta, \hat{\rho}_{\beta'}), \tag{5.4}$$

where $\hat{U}' = e^{-\mathrm{i}\hat{H}'\tau}$.

We may interpret (5.3) as telling us that the success probabilities of two different tasks are the same (cf. Fig. 5.1):

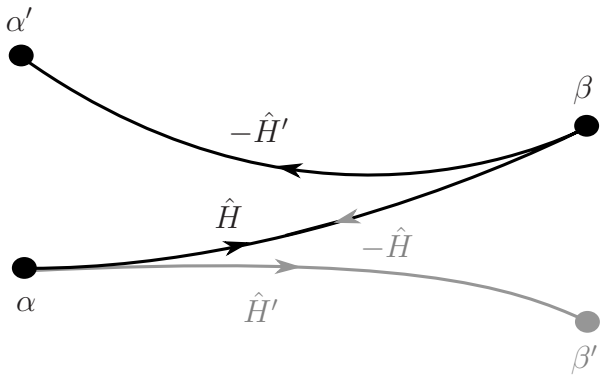

Figure 5.1: Schematic illustration of the state evolution of a closed system over a fixed time τ in Hilbert space, subject to the Hamiltonians as given. Loschmidt echo: $\alpha \to \beta \to \alpha'$; forward stability: $\alpha \to \beta$ versus $\alpha \to \beta'$.

1. Forward stability: The task to set up the generating Hamiltonian in such a way, that the system evolves from state α into given state β in time τ. The success probability is $F(\psi_\beta, \psi_{\beta'})$.

2. Loschmidt echo: The task to return to the initial state α in time τ from that state β by manipulating the Hamiltonian for the way back, with success probability $F(\psi_\alpha, \psi_{\alpha'})$

This implies for the asymmetry measure

$$\kappa = F(\psi_\beta, \psi_{\beta'}) - F(\psi_\alpha, \psi_{\alpha'}) = 0 \tag{5.5}$$

for any τ and any perturbation.

5.1.1 Fidelity Decay

Eq. (5.5) still does not tell us anything about the separate fidelities. The decay of the fidelity (5.3) for perturbed Hamiltonians has been widely investigated for different kind of models, initial states and perturbations [20]. For small perturbations the dynamical behavior of the fidelity of the Loschmidt echo,

$$F(t) = |\langle\psi| e^{\mathrm{i}\hat{H}'t} e^{-\mathrm{i}\hat{H}t} |\psi\rangle|^2, \tag{5.6}$$

where $|\psi\rangle$ is the initial state, can be calculated using first-order stationary perturbation theory [32], yielding

$$F(t) \approx \left| \sum_n c_n e^{-\mathrm{i}V_n \epsilon t} \right|^2, \tag{5.7}$$

where $V_n = \langle u_n | \hat{V} | u_n \rangle$ is the energy shift of eigenstate $|u_n\rangle$ of $\hat{H}$, and $c_n = |\langle u_n | \psi \rangle|^2$. $F(t)$ only depends on the initial state and on the perturbation, but is independent of the

Hamiltonian $\hat{H}$. To get the dynamical behavior for small times t, $F(t)$ can be expanded into a power series:

$$F(t) \approx 1 - (\Delta\hat{V})^2\epsilon^2 t^2 + \dots, \tag{5.8}$$

where

$$(\Delta\hat{V})^2 = \langle\psi|\hat{V}^2|\psi\rangle - \langle\psi|\hat{V}|\psi\rangle^2. \tag{5.9}$$

This shows that for small times, the fidelity decay is always quadratic in time.

For large t, the statistical behavior of $F(t)$ can be calculated [32]. From (5.7) we obtain

$$\begin{aligned} F(t) &= \sum_{n,m} c_n c_m cos((V_n - V_m)\epsilon t), \\ &= \bar{F} + \sum_{n,m}^{n\neq m} c_n c_m cos((V_n - V_m)\epsilon t), \end{aligned} \tag{5.10}$$

where $\bar{F} = \sum_n c_n^2$ is the time average of the fidelity. Now we take an ensemble average over different initial states and perturbations to obtain

$$\langle F(t)\rangle = \langle\bar{F}\rangle + \underbrace{\langle\sum_{n,m}^{n\neq m} c_n c_m\rangle}_{1-\langle\bar{S}\rangle}\langle cos((V_n - V_m)\epsilon t)\rangle \tag{5.11}$$

$$= \langle\bar{F}\rangle + (1 - \langle\bar{S}\rangle)\langle cos((V_n - V_m)\epsilon t)\rangle. \tag{5.12}$$

Thus the decay depends on the distribution of $V_n - V_m$, and if this distribution is Gaussian, also the decay law is Gaussian.

5.1.2 Bipartite Systems

The fidelity decay and (5.5) tell us that we can neither return to the initial state α by reversing the dynamics nor definitely reach any given state β by setting up the Hamiltonian, if there are perturbations. But, since $\kappa = 0$, there is no preferred direction in time: This is not surprising, because a system evolving in time under unitary dynamics does not show any typicality of states (there is no equilibrium state) [16]. Hence, we cannot yet see irreversibility based on this scenario.

For a small subsystem within a closed bipartite system, though, there is typicality of states (meaning that almost any state of the whole system - consistend with the macroscopic conditions - amounts to nearly the same state for the small subsystem) [16, 19]. Therefore, we partition the system into two subsystems, A and B. With subsystem A being the one of interest, the reduced states are given by (in the following, all these

density operators refer to reduced states of subsystem A only)

$$\hat{\rho}_\alpha = \mathrm{Tr_B}\left\{\hat{\rho}_{\mathrm{tot}}^{(\alpha)}\right\}, \tag{5.13}$$

$$\hat{\rho}_{\alpha'} = \mathrm{Tr_B}\left\{\hat{U}'(-\tau)\hat{U}(\tau)\hat{\rho}_{\mathrm{tot}}^{(\alpha)}\hat{U}^\dagger(\tau)\hat{U}'^\dagger(-\tau)\right\}, \tag{5.14}$$

$$\hat{\rho}_\beta = \mathrm{Tr_B}\left\{\hat{U}(\tau)\hat{\rho}_{\mathrm{tot}}^{(\alpha)}\hat{U}^\dagger(\tau)\right\}, \tag{5.15}$$

$$\hat{\rho}_{\beta'} = \mathrm{Tr_B}\left\{\hat{U}'(\tau)\hat{\rho}_{\mathrm{tot}}^{(\alpha)}\hat{U}'^\dagger(\tau)\right\}, \tag{5.16}$$

where $\hat{\rho}_{\mathrm{tot}}^{(\alpha)}$ is the initial state α of the total system, $\hat{U}(\tau) = e^{-\mathrm{i}\hat{H}t/\hbar}$ is the evolution operator of the unperturbed system, and $\hat{U}'(\tau) = e^{-\mathrm{i}\hat{H}'t/\hbar}$ is the evolution operator of the perturbed system.

What will happen if the system is subject to the same state evolution and control limits as above (cf. Fig. 5.1), but now from the view of subsystem A in its reduced Hilbert space? If subsystem A is small enough compared to B (i.e. the Hilbert-space dimensions fulfill $d_\mathrm{A} \ll d_\mathrm{B}$), we expect the initial state of the total system to relax into an equilibrium state $\hat{\rho}_\mathrm{eq}$ with respect to subsystem A, independently of the details of the interactions [16, 19, 24]. If the perturbation does not change the structure of the Hamiltonian (which we assume here), the states $\hat{\rho}_\beta$ and $\hat{\rho}_{\beta'}$ should be this equilibrium state for times τ larger than a typical relaxation time τ_relax:

$$\hat{\rho}_\beta \approx \hat{\rho}_{\beta'} \approx \hat{\rho}_\mathrm{eq} \qquad \text{for} \quad \tau > \tau_\mathrm{relax}. \tag{5.17}$$

Note that the condition $\hat{\rho}_\beta \approx \hat{\rho}_{\beta'}$ does not define τ_relax, and that τ_relax generally depends on the initial state and the details of the Hamiltonian (especially on the interaction strength between subsystems A and B), but should be nearly independent of the weak perturbation.

Because of the random perturbation, we expect the resulting state of the Loschmidt echo $\hat{\rho}_{\alpha'}$ to be some random state for large enough τ (which is most probably the equilibrium state in the subsystem), so that we can define an echo relaxation time τ_echo using

$$\hat{\rho}_{\alpha'} \approx \hat{\rho}_\mathrm{eq} \quad \Leftrightarrow \quad \tau > \tau_\mathrm{echo}. \tag{5.18}$$

where τ_echo mainly depends on the details of the perturbation, and is actually proportional to the perturbation strength ϵ (cf. Sec. 5.1.1). Therefore, τ_relax and τ_echo are not correlated (e.g. setting $\epsilon \to 0$ would lead to $\tau_\mathrm{echo} \to \infty$ without influencing τ_relax).

To analyze the stability of the dynamics from the view of the subsystem A, we compare the reduced states of the subsystem using

$$F_\mathrm{A} = F_\mathrm{A}(\hat{\rho}_\mathrm{A}, \hat{\sigma}_\mathrm{A}) = F_\mathrm{A}(\mathrm{Tr_B}\{\hat{\rho}_\mathrm{tot}\}, \mathrm{Tr_B}\{\hat{\sigma}_\mathrm{tot}\}), \tag{5.19}$$

where $\hat{\rho}_\mathrm{tot}$ refers to the state of the combined system, and which may be called "reduced" fidelity [42]. In particular, the following state distances are considered (cf. Fig. 5.1):

- $F_\mathrm{A}(\hat{\rho}_\beta, \hat{\rho}_{\beta'})$, telling us how stable the forward dynamics is. According to (5.17) we expect

$$F_\mathrm{A}(\hat{\rho}_\beta, \hat{\rho}_{\beta'}) \to 1 \qquad \text{for} \quad \tau > \tau_\mathrm{relax}. \tag{5.20}$$

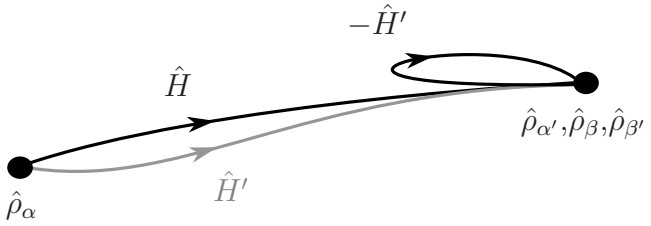

Figure 5.2: Schematic illustration of the state evolution in the reduced Hilbert space of subsystem A ($N_{\mathrm{A}} \ll N_{\mathrm{tot}}$) for $\tau > \tau_{\mathrm{echo}}$, subject to the Hamiltonians of the total system as indicated (cf. Fig. 5.1).

- $F_{\mathrm{A}}(\hat{\rho}_{\alpha}, \hat{\rho}_{\alpha'})$, which characterizes the Loschmidt echo and tells us how stable the dynamics of the subsystem is under reversion. According to (5.18) we obtain

$$F_{\mathrm{A}}(\hat{\rho}_{\alpha}, \hat{\rho}_{\alpha'}) \to 0 \;\; \Leftrightarrow \;\; \tau > \tau_{\mathrm{echo}}, \tag{5.21}$$

  provided the initial state α does not already produce a local equilibrium state, i.e. we require

$$F_{\mathrm{A}}(\hat{\rho}_{\alpha}, \hat{\rho}_{\beta}) \to 0 \;\; \Leftrightarrow \;\; \tau > \tau_{\mathrm{dyn}}. \tag{5.22}$$

  An echo may be called locally observable as long as $F_{\mathrm{A}}(\hat{\rho}_{\alpha}, \hat{\rho}_{\alpha'}) > F_{\mathrm{A}}(\hat{\rho}_{\alpha}, \hat{\rho}_{\beta})$.

- $F_{\mathrm{A}}(\hat{\rho}_{\beta}, \hat{\rho}_{\alpha'})$, characterizing how stable the reached state $\hat{\rho}_{\beta}$ is with respect to the reversal based on $\hat{H}'$.

The corresponding asymmetry measure is, generalizing (5.5),

$$\kappa_{\mathrm{A}} = F_{\mathrm{A}}(\hat{\rho}_{\beta}, \hat{\rho}_{\beta'}) - F_{\mathrm{A}}(\hat{\rho}_{\alpha}, \hat{\rho}_{\alpha'}). \tag{5.23}$$

Asymptotically for large times $\tau > \tau_{\mathrm{echo}}, \tau_{\mathrm{relax}}$ the two tasks defined above (in reference to (5.3)) have now almost opposite success probabilities, i.e. $\kappa_{\mathrm{A}} \approx 1$, cf. (5.20) and (5.21).

The asymmetry is the result of two features: Stable relaxation on the one hand side and limited resources of control for returning back to the initial state on the other hand side. Both these features are not independent, though: The resulting arrow of time reflects the fact that the insufficient control ($\epsilon \neq 0$) is counterbalanced by thermal relaxation in the forward, but not backward direction (cf. Fig. 5.2). Figure 5.2 is basically the same as Fig. 5.1: It shows schematically the state evolution over time τ, but now in the reduced Hilbert space of subsystem A only. Both the stable relaxation into equilibrium (black line with $\hat{H}$ and grey line with $\hat{H}'$) as well as the instability of the Loschmidt echo (black lines with $\hat{H}$ and $-\hat{H}'$) are shown. These two features characterize thermodynamical irreversibility. The directedness of the dynamics is clearly visible.

5.2 Numerical Studies

In the following, we apply this approach to a closed, homogeneous spin network ("quantum world") composed of $N_{\mathrm{tot}} = 13$ spins, while a variable number $N_{\mathrm{A}} < N_{\mathrm{tot}}$ of spins shall be the subsystem A of interest (Fig. 5.3). The respective Hilbert space dimensions are thus $d_{\mathrm{A}} = 2^{N_{\mathrm{A}}}$, $d_{\mathrm{B}} = 2^{N_{\mathrm{B}}}$. The network is taken to be structureless, so that partitions can, indeed, be taken at will, without any built-in preference.

The Hamiltonian of the system is

$$\hat{H} = \hat{H}_0 + a\hat{H}_{\mathrm{I}} \tag{5.24}$$

where $\hat{H}_0$ is the energy of the noninteracting spins (with energy splitting $\omega = 1$)

$$\hat{H}_0 = \hat{H}_{\mathrm{A}} + \hat{H}_{\mathrm{B}} = \sum_{i=1}^{N_{\mathrm{tot}}} \frac{1}{2}\hat{\sigma}_z^{(i)}, \tag{5.25}$$

$\hat{H}_{\mathrm{I}}$ is the interaction between the spins and a is a coupling parameter. In our present model the parameter a sets the scale for τ_{relax} (for N_{A} small enough compared to N_{tot}) and τ_{dyn}. We set $a = 0.001$, so that the weak coupling condition should be fulfilled.

For the choice of the interaction between the spins, we can use the same considerations as in Sec. 3.1: By demanding

$$[\hat{H}_0, \hat{H}_I] = 0, \tag{5.26}$$

the total Hilbert space is divided into uncoupled eigenspaces of $\hat{H}_0$, which then is a conserved quantity. Eq. (5.26) is fullfilled, if $\hat{H}_I$ is block diagonal in the eigenbasis of

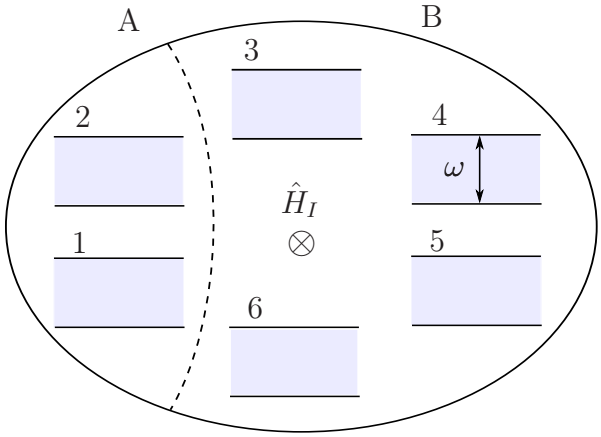

Figure 5.3: Schematic structure of the model (here $N_{\mathrm{tot}} = 6$, $N_{\mathrm{A}} = 2$). The dashed line indicates the partition into subsystems A, B.

$\hat{H}_0$:

$$\hat{H}_I = \sum_s \sum_{i,i'} (\hat{H}_I^{(s)})_{ii'} |s;i\rangle\langle s;i'| = \begin{pmatrix} \hat{H}_I^{(1)} & \cdots & 0 \\ & \hat{H}_I^{(2)} & \\ \vdots & \ddots & \vdots \\ & & \hat{H}_I^{(s)} \\ 0 & \cdots & \ddots \end{pmatrix}, \tag{5.27}$$

where s denotes the eigenvalues of $\hat{H}_0$, i and i' the respective eigenstates, and $(\hat{H}_I^{(s)})_{ii'}$ the matrix elements of the interaction. The blocks $\hat{H}_I^{(s)}$ are chosen to be random hermitian matrices from the Gaussian unitary ensemble (cf. Sec. 2.4). The total Hamiltonian $\hat{H}$ also has this block diagonal structure, because $\hat{H}_0$ is, of course, diagonal in its eigenbasis. This way, only states which lie within the same eigenspace of $\hat{H}_0$ are coupled, and by choosing the initial state to totally lie within such an eigenspace denoted by s,

$$\hat{\rho}_0 = \sum_{j,j'} (\hat{\rho}_s)_{jj'} |s,j\rangle\langle s,j'|, \tag{5.28}$$

we only have to consider this eigenspace rather than the total Hilbert space for calculating the dynamics.

With (5.1) we essentially stick to a global control referring to subsystem A and its environment B. Since the only requirement for $\hat{V}$ is that it does not essentially change the structure of the Hamiltonian (e.g. by turning a microcanonical interaction into a canonical one), we take

$$\hat{V} = \hat{V}_0 + a\hat{V}_\mathrm{I}, \tag{5.29}$$

where $\hat{V}_0$ is a diagonal matrix (in the eigenbasis of $\hat{H}_0$) with Gaussian distributed random numbers, a is defined in (5.24) and $\hat{V}_\mathrm{I}$ is a random matrix with the same structure as $\hat{H}_\mathrm{I}$. The perturbation strength according to (5.1) is set to $\epsilon = 0.01$, where a is defined in (5.24).

5.2.1 Behavior of the Reduced Fidelity

The initial state is taken to be a product state of single spin states with 7 spins excited and the other 6 being in the ground state. This way, the dynamics take place in the largest eigenspace - 1716 dimensions - of $\hat{H}_0$. Other initial states (see below) within this eigenspace subject to (5.22) could also be taken. Firstly, we investigate the reduced state of a subsystem A consisting of $N_A = 4$ spins. Such a subsystem is small compared to the environment (the rest of the spins), $d_\mathrm{A} \ll d_\mathrm{B}$, but still not too small, because for very small subsystems, there is in general a rather high probability (fidelity) to find the subsystem in its initial state (cf. App. C).

In Fig. 5.4 the fidelity measurements (according to Sec. 5.1.2) depending on the evolution time τ are shown. We can see that the qualitative theoretical expectations are confirmed by our numerical results. In this case, we found $a\tau_\mathrm{relax} \approx a\tau_\mathrm{dyn} \approx 0.03$ and $a\tau_\mathrm{echo} \approx 0.5$, which means that for times $\tau < \tau_\mathrm{echo}$ an echo is observable. For $\tau > \tau_\mathrm{echo}$, the state $\hat{\rho}_\beta$ is stable towards our attempt of reversal, cf. Fig. 5.2.

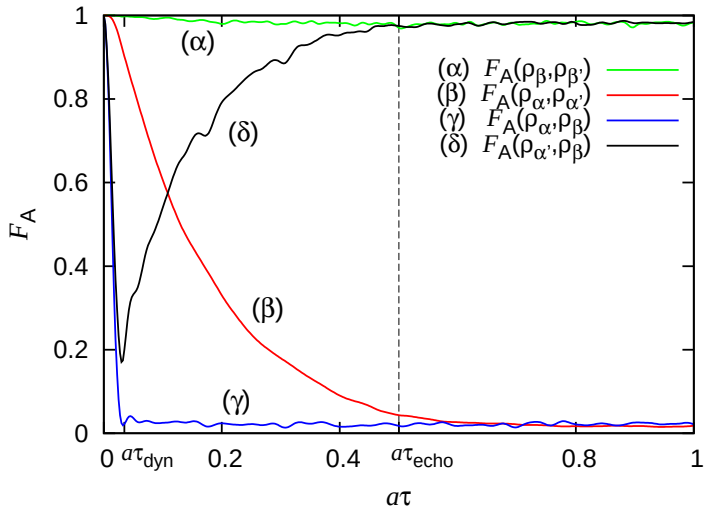

Figure 5.4: Reduced fidelity F_A between different state pairs (cf. Figs. 5.1 and 5.3) of subsystem A consisting of $N_\mathrm{A} = 4$ spins ($N_\mathrm{tot} = 13$), depending on the evolution time τ.

An echo might be present even for $\tau_\mathrm{echo} > \tau > \tau_\mathrm{relax}$, i.e. even after a thermal state has been reached for A. This is possible because the backward control has been assumed to be global, i.e. operating on the total system. The memory of the initial state is, of course, still available in the system, even though we only focus on subsystem A.

Maximally entangled initial state

Another, interesting initial state is a maximally entangled state between subsystem A and the rest of the system. We again investigate a system with a total of $N_\mathrm{tot} = 13$ spins. The initial state is chosen to be a EPR-like state for 6 of the spins, and the rest of the spins is in the ground state:

$$|\psi\rangle = \sum_{\sigma_z=3} \prod_{i=1}^{6} |m_i\rangle \otimes \prod_{i=7}^{13} |m_i = 0\rangle, \tag{5.30}$$

where $m_i = 0, 1$ is the state of spin i (0: groundstate, 1: excited state), the condition $\sigma_z = 3$ of the sum means all possible states of the first 6 spins such that exactly 3 spins are excited ($\sum_{i=1}^{6} m_i = 3$), and $\prod$ indicates a sequence of tensor products.

The subsystem A here are the first 3 spins ($i = 1, 2, 3$). Initially, the reduced state of A is a maximally mixed state, i.e. has the highest possible entropy (minimum purity). During the evolution of the total system, this local entropy can only decrease ($\rightarrow$ increase of purity). Since the state of the total system is pure, also the local entropy of the rest of the system will decrease [2]. Nethertheless, similar results as above for the reduced fidelity of subsystem A can be obtained, cf. Fig. 5.5. Figure 5.6 shows the increase of purity in subsystem A. In Fig. 5.5 (a), the fidelities $F_\mathrm{A}(\hat{\rho}_\alpha, \hat{\rho}_{\alpha'})$ and $F_\mathrm{A}(\hat{\rho}_\alpha, \hat{\rho}_\beta)$ are unequal zero, because the local initial state already is a mixed state, which is similar

to the equilibrium state (the fidelity between initial state and equilibrium state is not zero).

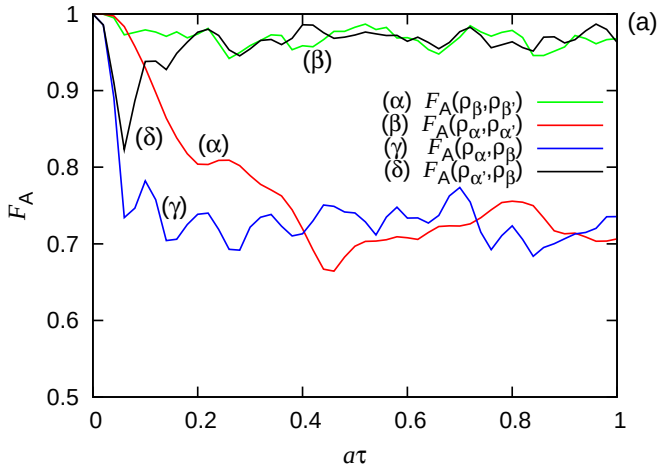

Figure 5.5: Reduced fidelity F_A depending on the evolution time τ (cf. Fig. 5.4, note the different scale of the y-axis), for an initial EPR-like state and with $N_A = 3$ spins ($N_{tot} = 13$).

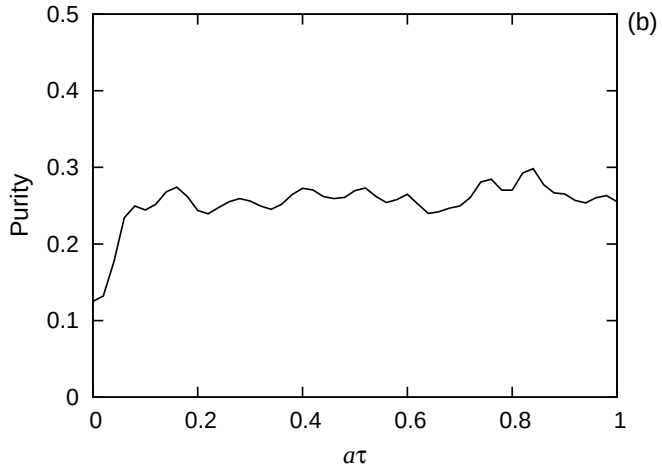

Figure 5.6: Purity of state $\hat{\rho}_\beta$ for an initial EPR-like state (cf. Fig. 5.5.

5.2.2 Emergence of Irreversibility

In the following, we show how irreversibility, $\kappa_A \approx 1$, emerges under global control from an appropriate partitioning of the closed system into an observed, small subsystem A and the rest of the total system. For this purpose, we investigate the reduced state of subsystem A with different sizes, while the whole system is always the same, with the

initial state as given above (cf. Sec. 5.2.1). Low values of κ_A indicate that there is no asymmetry, i.e. no preferred direction in time.

Figure 5.7 exemplifies the trend of κ_A for N_A approaching N_{tot}. Figure 5.8 summarizes our results. The behavior for small N_A (small d_A) is due to the rather high probability to find subsystem A in its initial state, i.e. $F_A(\hat{\rho}_\alpha, \hat{\rho}_{\alpha'}) \approx 1/d_A$. The limit $N_A = N_{tot}$ is again the non-partitioned system, not showing any preferred direction of the state evolution: (5.3) and thus $\kappa_A = 0$ is fulfilled for $\tau > \tau_{echo}$.

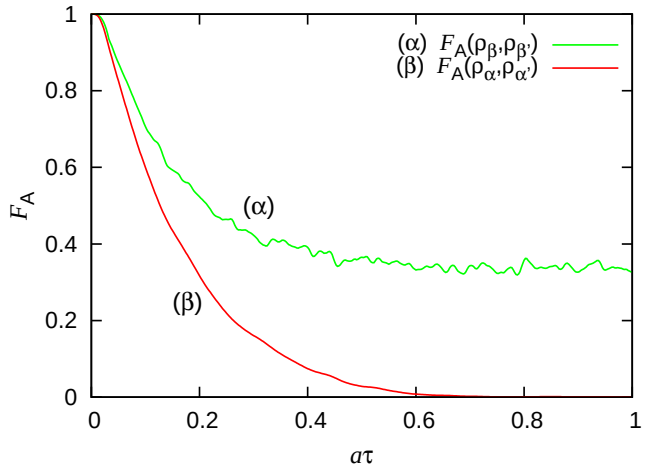

Figure 5.7: As Fig. 5.4, but now for subsystem A consisting of $N_A = 7$ spins. The low value of $F_A(\hat{\rho}_\beta, \hat{\rho}_{\beta'})$ shows that there is no longer a stable relaxation into an equilibrium state. Here, $\kappa_A \approx 0.35$.

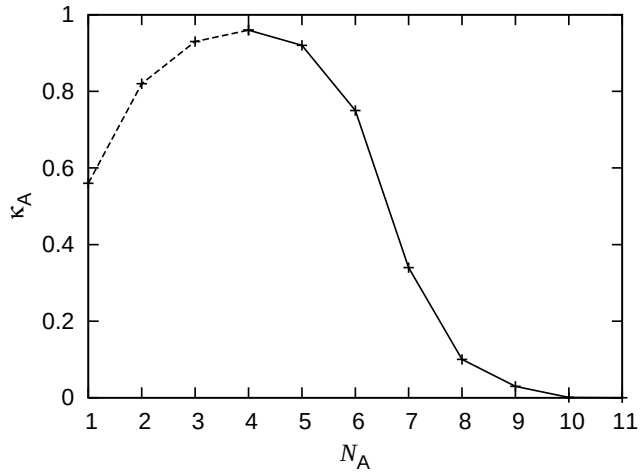

Figure 5.8: Asymmetry measure κ_A for $\tau > \tau_{echo}$ and for subsystem A consisting of N_A spins ($N_{tot} = 13$). The behavior for very small N_A (dashed) is explained in the text.

5.2.3 Reduced Fidelity for Local Control

We have seen that the Loschmidt echo remains observable for $\tau < \tau_{\text{echo}}$, if we allow global control with a small, global error (homogeneous control) over the system, but only focus on the dynamics of a subsystem. From this point of view, it seems as if this is a violation of the second law. But within the total, closed system, there is no loss of information, the entropy stays constant.

Here, we limit our control on only the subsystem, but without any error (inhomogeneous control), and compare $F_{\text{A}}(\hat{\rho}_\alpha, \hat{\rho}_{\alpha'})$ (Loschmidt echo) with $F_{\text{A}}(\hat{\rho}_\alpha, \hat{\rho}_\beta)$ (dynamics). The total system, though, is described by the same structureless Hamiltonian as above.

To carry out this local reversal, we first have to split the Hamiltonian into

$$\hat{H} = \hat{H}_{\text{A}} + \hat{H}_{\text{B}} + \hat{H}_{\text{AB}}, \tag{5.31}$$

where

$$\hat{H}_{\text{A}} = \sum_i \hat{Q}_{\text{A},i} \text{Tr}\{\hat{Q}^\dagger_{\text{A},i} \hat{H}\}, \tag{5.32}$$

and where the $\hat{Q}_{\text{A},i}$ are all orthogonal and normalized operators of the total Hilbert space, which only act on the subsystem A of interest. All these operators can be calculated by

$$\hat{Q}_{\text{A}} = \sqrt{2^{-N_{\text{tot}}}} \hat{\sigma}^{(1)}_{i_1} \otimes \hat{\sigma}^{(2)}_{i_2} \otimes \cdots \otimes \hat{\sigma}^{N_{\text{A}}}_{i_{N_{\text{A}}}} \otimes \mathbb{1}_{\text{B}}, \tag{5.33}$$

where $\sqrt{2^{-N_{\text{tot}}}}$ is a normalization factor, $i_n = 1, x, y, z$, and $\hat{\sigma}^{(n)}_{i_n}$ are the Pauli operators acting only on spin n ($\hat{\sigma}_1 = \mathbb{1}$ shall be a unit operator). $\mathbb{1}_{\text{B}}$ is the unit operator acting on $\mathcal{H}_{\text{B}}$.

The reversal process is now defined as

$$\hat{H} \to -\hat{H}' = -\hat{H}_{\text{A}} + \hat{H}_{\text{B}} + \hat{H}_{\text{AB}} = \hat{H} - 2\hat{H}_{\text{A}}. \tag{5.34}$$

Because of the high numerical effort needed for solving (5.33), we consider a spin network consisting of $N_{\text{tot}} = 8$ spins only. Otherwise the total Hamiltonian is the same as above (Sec. 5.2). The initial state is a product state with 4 spins excited and the other 4 being in the ground state.

To see whether an echo may be observed, we compare $F_{\text{A}}(\hat{\rho}_\alpha, \hat{\rho}_{\alpha'})$ with $F_{\text{A}}(\hat{\rho}_\alpha, \hat{\rho}_\beta)$. Calculating $F_{\text{A}}(\hat{\rho}_\beta, \hat{\rho}_{\beta'})$ does not give the expected result here: The "perturbation" ($\hat{V} = \hat{H}' - \hat{H}$) of the Hamiltonian is of the same order of magnitude as the Hamiltonian, and because of the small size of the system, there is no stable relaxation as in Sec. 5.2.1 ($F_{\text{A}}(\hat{\rho}_\beta, \hat{\rho}_{\beta'}) = 1$ was only observed for $N_{\text{A}} = 1$, which is too small for our purposes, cf. Sec. 5.2.1). Figure 5.9 shows the reduced fidelity of the Loschmidt echo ($F_{\text{A}}(\hat{\rho}_\alpha, \hat{\rho}_{\alpha'})$) and of the dynamics ($F_{\text{A}}(\hat{\rho}_\alpha, \hat{\rho}_\beta)$), for (a) $N_{\text{A}} = 3$ and (b) $N_{\text{A}} = 7$ spins. We find that in all these cases $\tau_{\text{echo}} \approx \tau_{\text{dyn}}$, so that there is no time window for observing an echo. Actually, the control over the Hamiltonian is very limited, even if $N_{\text{A}} = 7$. As we can see in (5.33), only one fourth of all basis operators of the total Hamiltonian are controlled. This may explain why the two Figs. 5.9 (a) and (b) look nearly the same: In both cases, the influence of the reversal is very weak.

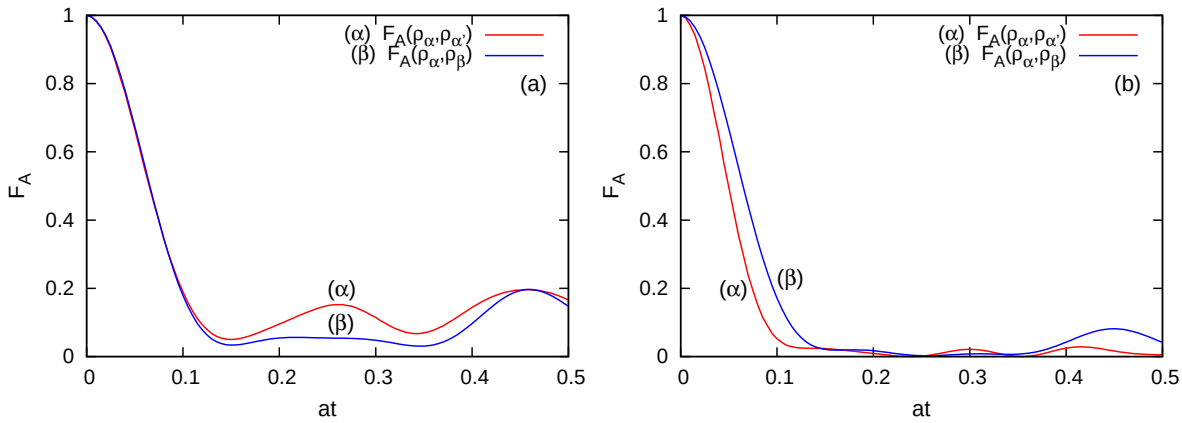

Figure 5.9: Reduced fidelity decay of the Loschmidt echo $F_{\mathrm{A}}(\hat{\rho}_{\alpha}, \hat{\rho}_{\alpha'})$ for local control compared with the dynamics $F_{\mathrm{A}}(\hat{\rho}_{\alpha}, \hat{\rho}_{\beta})$ for $N_{\mathrm{tot}} = 8$ spins, (a) $N_{\mathrm{A}} = 3$ and (b) $N_{\mathrm{A}} = 7$ spins.

6 Summary

We have investigated a closed laser model subject to pure Schrödinger dynamics. The model consisted of the three basic elements of a laser: One resonant mode of the radiation field inside an optical cavity represented by a harmonic oscillator, the gain medium represented by a non-degenerate two-level system (spin) interacting resonantly with the field mode, and the energy pump modeled by embedding the interfacing spin within a finite spin network with an energy exchange condition.

Depending on the initial state, three special scenarios have been addressed: Lasing relaxation, non-lasing relaxation and energy back-flow from the field mode. The respective local equilibrium states were in accord with the theory of quantum thermodynamics. The agreement of the numerical results with the thermodynamical expectations is quite good, considering the relatively small size of the spin network.

For the lasing relaxation, the spin network was set up in the highest energy eigenstate and the field mode in the ground state. We have seen that during relaxation the field mode of our laser model is in a phase-diffused Glauber state, even for a random interaction between the gain medium and pump reservoir, so that in principle coherent pumping was possible. The result of the LEMBAS analysis is consistent with this finding: The energy change of the field mode is induced by heat flow only, i.e. the effective dynamics of the field mode induced by the environment is incoherent.

For the energy back-flow, the spin network was initially in the ground state, while the field mode was (i) in a phase-diffused Glauber state and (ii) in a coherent Glauber state. The total energy flow was the same in both cases. The analysis with LEMBAS, however, yielded different results. The reason for this may be that for quantum systems, the concept of local entropy and its change (and thus of heat and work flows) depends on the partition used.

We have seen that it is thermodynamically possible to (partly) extract energy from the field mode in the phase-diffused Glauber state, and, without any other effect, perform the same amount of work on another system. This generally applies to systems, which are not in a thermal state. Nevertheless, it is unclear how and whether this possibility can be practically used.

Relaxation is not yet the full story: In chapter 5, we have investigated why this process cannot be inverted. We we have seen that the arrow of time in a quantum system with unitary dynamics is not an absolute property of the system but rather a consequence of two externally imposed conditions: (i) The system is subject to Hamiltonian perturbations, caused by limited control over the system when carrying out the Loschmidt echo. (ii) Within the system one focuses on a small enough part A (thus allowing for local relaxation).

In order to characterize both instability and irreversibility, we have applied fidelity

measurements subject to perturbations. We introduced an asymmetry measure comparing the stability of the forward dynamics with the stability of the Loschmidt echo, and have seen that perturbations and local observation lead to a time-asymmetric evolution.

This approach has been applied to a spin network (the "matter"-part of our quantum-optical scenario) by focusing on part of the spins forming a subsystem, but nevertheless allowing global, imperfect control. This simplified model has the advantage of homogeneity, i.e. we can choose partitions at will without having to consider physical constraints (e.g. like oscillator versus spin in the laser model)

We found that there is a time window for which an echo is observable, but asymptotically for large times the reached state is stable towards our attempt of reversal. By reducing the size of the subsystem, we have seen the emergence of a local time's arrow and therewith irreversibility within total systems as small as some 10 spins.

Finally, we have limited our control to a local reversal (sign-flip) of the Hamiltonian of the observed subsystem only. In this case, we found that there is no observable echo at all.

A Commutation Relation of the Jaynes-Cummings Interaction

The total Jaynes-Cummings Hamiltonian for the interaction of a two-level atom with one mode of the quantized radiation field is (cf. Sec. 2.2.2, here for $g = 1$)

$$\hat{H} = \hat{H}_{\mathrm{A}} + \hat{H}_{\mathrm{F}} + \hat{V}_{\mathrm{JC}} = \frac{\omega}{2}\hat{\sigma}_z + \nu\hat{N} + \hat{\sigma}_-\hat{a}^\dagger + \hat{\sigma}_+\hat{a}. \tag{A.1}$$

Using the commutation relations

$$[\hat{\sigma}_z, \hat{\sigma}_\pm] = \pm 2\hat{\sigma}_\pm, \tag{A.2}$$

$$\left[\hat{N}, \hat{a}\right] = -\hat{a}, \tag{A.3}$$

$$\left[\hat{N}, \hat{a}^\dagger\right] = \hat{a}^\dagger, \tag{A.4}$$

and remembering that operators, which act on different Hilbert spaces, always commute, we can calculate the commutator

$$\begin{aligned}
\left[\hat{H}_{\mathrm{A}} + \hat{H}_{\mathrm{F}}, \hat{V}_{\mathrm{JC}}\right] &= \left[\frac{\omega}{2}\hat{\sigma}_z, \hat{\sigma}_-\hat{a}^\dagger\right] + \left[\frac{\omega}{2}\hat{\sigma}_z, \hat{\sigma}_+\hat{a}\right] + \left[\nu\hat{N}, \hat{\sigma}_-\hat{a}^\dagger\right] + \left[\nu\hat{N}, \hat{\sigma}_+\hat{a}\right] && \text{(A.5)}\\
&= -\omega\hat{\sigma}_-\hat{a}^\dagger + \omega\hat{\sigma}_+\hat{a} + \nu\hat{\sigma}_-\hat{a}^\dagger - \nu\hat{\sigma}_+\hat{a} && \text{(A.6)}\\
&= (\nu - \omega)\hat{\sigma}_-\hat{a}^\dagger + (\omega - \nu)\hat{\sigma}_+\hat{a}. && \text{(A.7)}
\end{aligned}$$

If $\omega = \nu$ we obtain

$$\left[\hat{H}_{\mathrm{A}} + \hat{H}_{\mathrm{F}}, \hat{V}_{\mathrm{JC}}\right] = 0. \tag{A.8}$$

B Poisson and Thermal Distribution with the Same Entropy

The Poisson distribution for a harmonic oscillator is given by

$$P_{\text{Poiss}}(n) = e^{-\langle \hat{N} \rangle} \frac{\langle \hat{N} \rangle^n}{n!}, \tag{B.1}$$

where $n = 0, 1, ..., \infty$ denotes the eigenstates of the number operator $\hat{N}$, and $P_{\text{Poiss}}(n)$ is the probability to find the oscillator in state n. The thermal distribution is given by

$$P_{\text{th}}(n) = \frac{1}{Z} e^{-\beta \hbar \omega n}, \tag{B.2}$$

where β is the inverse temperature, ω the eigenfrequency of the oscillator and $Z = \sum_n e^{-\beta \hbar \omega n}$ is a normalization factor.

We will now calculate how to set the inverse temperature β, such that the thermal distribution and the Poissonian distribution with given $\langle \hat{N} \rangle$ have the same von Neumann entropy. To get this inverse temperature, we solve $S(P_{\text{th}})$ for β and set $S(P_{\text{th}}) = S(P_{\text{Poiss}})$. The von Neumann entropy of the thermal distribution is (with $\hbar\omega = 1$ and $k_B = 1$)

$$\begin{aligned} S(P_{\text{th}}) &= -\sum_n P_{\text{th}}(n) \ln\left(P_{\text{th}}(n)\right) && \text{(B.3)} \\ &= -\sum_n \frac{e^{-\beta n}}{Z} \ln\left(\frac{e^{-\beta n}}{Z}\right) && \text{(B.4)} \\ &= \frac{1}{Z} \sum_n e^{-\beta n} \left(\ln(Z) + \beta n\right) && \text{(B.5)} \\ &= \frac{1}{Z} \left(Z \ln(Z) + \sum_n \beta n e^{-\beta n} \right) && \text{(B.6)} \\ &= \ln(Z) + \frac{1}{Z} \sum_n \beta n e^{-\beta n}. && \text{(B.7)} \end{aligned}$$

Now we use $Z = \sum_n e^{-\beta n} = \frac{e^\beta}{e^\beta - 1}$ and $\sum_n \beta n e^{-\beta n} = \frac{\beta e^\beta}{(e^\beta - 1)^2}$:

$$\begin{aligned} S(P_{\text{th}}) &= \ln\left(\frac{e^\beta}{e^\beta - 1}\right) + \frac{e^\beta - 1}{e^\beta} \frac{\beta e^\beta}{(e^\beta - 1)^2} && \text{(B.8)} \\ &= \beta - \ln\left(e^\beta - 1\right) + \frac{\beta}{e^\beta - 1} && \text{(B.9)} \\ &= \frac{\beta e^\beta}{e^\beta - 1} - \ln\left(e^\beta - 1\right), && \text{(B.10)} \end{aligned}$$

which can only be solved numerically for β. For $\hbar\omega \neq 1$ we would obtain $\beta' = \frac{\beta}{\hbar\omega}$

C Appendix on Fidelity

Here we calculate how the fidelity of the Loschmidt echo in a subsystem of a bipartite system statictically behaves, depending on the number of dimensions N of the subsystem. The initial state $|\alpha\rangle$ given in some basis $\{|u_i\rangle\}$ of the subsystem is

$$|\alpha\rangle = \sum_i^N c_i |u_i\rangle, \qquad \text{with } \sum_i^N |c_i|^2 = 1. \tag{C.1}$$

After the echo, the subsystem generally is in a mixed state

$$\hat{\rho} = \sum_{i,j}^N p_{ij} |u_i\rangle\langle u_j|, \qquad \text{with } \sum_i^N p_{ii} = 1. \tag{C.2}$$

The fidelity between these states is

$$\begin{aligned} F &= \langle\alpha|\hat{\rho}|\alpha\rangle \\ &= \sum_{i,j,m,n}^N c_i^* c_j p_{mn} \langle u_i|u_m\rangle\langle u_n|u_j\rangle \\ &= \sum_{i,j}^N c_i^* c_j p_{ij}. \end{aligned} \tag{C.3}$$

By averaging ($\| \; \|$) either over (i) a uniform distribution of initial states,

$$\|c_i^* c_j\| = \frac{1}{N}\delta_{ij}, \tag{C.4}$$

or over (ii) a uniform distribution of mixed states $\hat{\rho}$,

$$\|p_{ij}\| = \frac{1}{N}\delta_{ij}, \tag{C.5}$$

yields the same result for the fidelity:

$$\text{(i)} \quad \|F\| = \sum_{i,j}^N \|c_i^* c_j\| p_{ii} = \sum_i^N \frac{1}{N} p_{ii} = \frac{1}{N} \tag{C.6}$$

$$\text{(ii)} \quad \|F\| = \sum_{i,j}^N c_i^* c_j \|p_{ij}\| = \sum_i^N \frac{1}{N} |c_i|^2 = \frac{1}{N}. \tag{C.7}$$

This shows that for very small subsystems this fidelity may be considerably larger than zero.

Bibliography

[1] Robert Alicki. The quantum open system as a model of the heat engine. *J. Phys. A: Math. Gen.*, 12:L103, 1979.

[2] Huzihiro Araki and Elliott H. Lieb. Entropy Inequalities. *Comm. math. Phys.*, 18:160, 1970.

[3] P. Borowski, J. Gemmer, and G. Mahler. Relaxation into equilibrium under pure Schrödinger dynamics. *Eur. Phys. J. B*, 35:255, 2003.

[4] E. Boukobza and D. J. Tannor. Termodynamics of bipartite systems: Application to light-matter interactions. *Phys. Rev. A*, 74(063823), 2006.

[5] E. Boukobza and D. J. Tannor. Three-level systems as amplifiers and attenuators: A thermodynamic analysis. *Phys. Rev. Lett.*, 98:240601, 2007.

[6] Patrizia Castiglione, Massimo Falcioni, Annick Lesne, and Angelo Vulpiani. *Chaos and Coarse Graining in Statistical Mechanics*. Campridge University Press, 2008.

[7] Claude Cohen-Tannoudji, Bernard Diu, and Franck Laloë. *Quantum Mechanics Volume I*. Hermann, second edition.

[8] Claude Cohen-Tannoudji, Bernard Diu, and Franck Laloë. *Quantum Mechanics Volume II*. Hermann, second edition.

[9] D. G. Cory, R. Laflamme, E. Knill, L. Viola, T. F. Havel, N. Boulant, G. Boutis, E. Fortunato, S. Lloyd, R. Martinez, C. Negrevergne, M. Pravia, Y. Sharf, G. Teklemariam, Y. S. Weinstein, and W. H. Zurek. NMR based quantum information processing: Achievements and prospects. *Fortschr. Phys.*, 48:875, 2000.

[10] Gavin E. Crooks. Quantum operation time reversal. *Phys. Rev. A*, 77:034101, 2008.

[11] James P. Crutchfield, Christopher J. Ellison, and John R. Mahoney. Time's barbed arrow: Irreversibility, crypticity, and stored information. *Phys. Rev. Lett.*, 103:094101, 2009.

[12] Wolfgang Demtröder. *Laser Spectroscopy*. Springer, third edition.

[13] Massimiliano Esposito, Katja Lindenberg, and Christian Van den Broeck. Universality of Efficiency at Maximum Power. *Phys. Rev. Lett.*, 102:130602, 2009.

[14] Edward H. Feng and Gavin E. Crooks. Length of time's arrow. *Phys. Rev. Lett.*, 101:090602, 2008.

[15] Yan V. Fyodorov. Introduction to the random matrix theory: Gaussian unitary ensemble and beyond. *arXiv:math-ph/0412017v1*, 2004.

[16] J. Gemmer, M. Michel, and G. Mahler. *Quantum Thermodynamics*. Springer Verlag, 2005.

[17] Christopher Gerry and Peter Knight. *Introductory Quantum Optics*. Cambridge University Press, first edition.

[18] Roy J. Glauber. Coherent and incoherent state of the radiation field. *Phys. Rev.*, 131:2766, 1963.

[19] Sheldon Goldstein, Joel L. Lebowitz, Roderich Tumulka, and Nino Zanghí. Canonical typicality. *Phys. Rev. Lett.*, 96:050403, 2006.

[20] T. Gorin, T. Prosen, T. H. Seligman, and M. Žnidarič. Dynamics of Loschmidt echoes and fidelity decay. *Physics Reports*, 435:33–156, 2006.

[21] E. L. Hahn. Spin echoes. *Phys. Rev.*, 80(4):580, 1950.

[22] Richard Jozsa. Fidelity for mixed quantum states. *J. Mod. Opt.*, 41:2315, 1994.

[23] P. T. Landsberg. Heat engines and heat pumps at positive and negative absolute temperatures. *J. Phys. A: Math. Gen.*, 10(10):1773, 1977.

[24] Noah Linden, Sandu Popescu, Anthony J. Short, and Andreas Winter. Quantum mechanical evolution towards thermal equilibrium. *arXiv:0812.2385v1*, 2008.

[25] J. J. Loschmidt. Über den Zustand des Wärmegleichgewichtes eines Systems von Körpern mit Rücksicht auf die Schwerkraft. *Wiener Ber.*, 73:128, 1876.

[26] Lorenzo Maccone. Quantum solution to the arrow-of-time dilemma. *Phys. Rev. Lett.*, 103:080401, 2009.

[27] M. C. Mackey. *Time's Arrow*. Springer, 1992.

[28] Günter Mahler and Volker A. WeberruÃ§. *Quantum Networks âĂŞ Dynamics of Open Nanostructures*. Springer Verlag, 1998.

[29] G. A. Melkov, A. A. Serga, V. S. Tiberkevich, A. N. Oliynyk, and A. N. Slavin. Wave front reversal of a dipolar spin wave pulse in a nonstationary three-wave parametric interaction. *Phys. Rev. Lett.*, 84:3438, 2000.

[30] Klaus Mølmer. Optical coherence: A convenient fiction. *Phys. Rev. A*, 55(4), 1997.

[31] Kae Nemoto and Samuel L. Braunstein. Quantum coherence: Myth or fact? *Phys. Lett. A*, 333:378, 2004.

[32] A. Peres. Stability of quantum motion in chaotic and regular systems. *Phys. Rev. A*, 30:1610, 1984.

[33] Sandu Popescu, Anthony J. Short, and Andreas Winter. Entanglement and the foundations of statistical mechanics. *Nature Physics*, 2:754, 2006.

[34] N. F. Ramsey. Thermodynamics and statistical mechanics at negative absolute temperatures. *Phys. Rev.*, 103(1):20, 1956.

[35] Terry Rudolph and Barry C. Sanders. Requirement of optical coherence for continuous-varibale quantum teleportation. *Phys. Rev. Lett.*, 87:077903, 2001.

[36] Harry Schmidt. *Thermal and Nonthermal Properties of Closed Bipartite Quantum Systems*. PhD thesis, Universität Stuttgart, 2007.

[37] Harry Schmidt and Günter Mahler. Control of local relaxation behavior in closed bipartite quantum systems. *Phys. Rev. E*, 72:016117, 2005.

[38] Harry Schmidt and Günter Mahler. Nonthermal equilibrium states of closed bipartite systems. *Phys. Rev. E*, 75:061111, 2007.

[39] Franz Schwabl. *Statistische Mechanik*. Springer, 2000.

[40] H. E. D. Scovil and E. O. Schulz-DuBois. Three-level masers as heat enginges. *Phys. Rev. Lett.*, 2(6), 1959.

[41] Marlan O. Scully and M. Suhail Zubairy. *Quantum Optics*. Cambridge University Press, sixth edition.

[42] Marco Žnidarič and Tomaž Prosen. Fidelity and purity decay in weakly coupled composite systems. *J. Phys. A: Math. Gen.*, 36:2463–2481, 2003.

[43] Gerald Waldherr and Günter Mahler. Emergence of irreversibility in quantum systems. *In preparation*, 2009.

[44] Gerald Waldherr and Günter Mahler. Lasing process in a closed bipartite quantum system: A thermodynamical analysis. *In preparation*, 2009.

[45] J. S. Waugh, W.-K. Rhim, and A. Pines. Spin echoes and loschmidt's paradox. *Pure Appl. Chem.*, 32:317, 1972.

[46] H. Weimer, M. J. Henrich, F. Rempp, H. Schröder, and G. Mahler. Local effective dynamics of quantum systmes: A generalized approach to work and heat. *EPL*, 83(30008), 2008.

[47] M. Youssef, G. Mahler, and A.-S. F. Obada. Quantum optical thermodynamic machines: Lasing as relaxation. 2009.

Danksagung

Als erstes möchte ich mich bei Prof. Dr. Günter Mahler sehr herzlich bedanken für die Betreuung meiner Diplomarbeit, für sein Interesse und für seine richtungsweisenden Vorschläge zu meiner Arbeit.

Mein Dank geht auch an Prof. Dr. Hans-Rainer Trebin für die Übernahme des Zweitberichts meiner Diplomarbeit.

Bedanken möchte ich mich bei den Institutsmitgliedern Heiko Schröder, Kilian Rambach, Jens Teifel, Hendrick Weimer, Thomas Jahnke, Suzanne Lanery und Pedro Vidal für hilfreiche Diskussionen und für ein angenehmes Arbeitsklima. Besonders bedanke ich mich bei Heiko Schröder, den ich vor allem zu Anfang meiner Diplomarbeit jederzeit mit technischen und physikalischen Fragen befallen habe, und bei Kilian Rambach für interessante physikalische Diskussionen.

Ein kleines Dankeschön gebührt auch Florian Rempp, der für kurzweilige Beschäftigung während der Mittagspausen gesorgt hat, die ich schon bald vermissen werde.

Bei Matthias Steiner, Stefan Rau, Adam Bühler und Matthias Zimmer bedanke ich mich für abwechslungsreiche Kaffeepausen und für schöne Zeiten während des Studiums.

Für ihre vielseitige Untestützung wärend meines gesamten Studiums danke ich meinen Eltern Sigrid und Albin Waldherr.

Bei meiner Frau Ling Waldherr bedanke ich mich dafür, dass sie immer für mich da ist. Dank ihr ist mir diese Arbeit oft leichter gefallen.